Master's Thesis
석사 학위논문

Artificial Tactile Sensor based on Pressure & Temperature Hybrid Sensing System for Thermal Detection

Minsoo Kang(강 민 수 姜 敏 洙)

Department of Information and Communication Engineering

DGIST

2021

Master's Thesis
석사 학위논문

Artificial Tactile Sensor based on Pressure & Temperature Hybrid Sensing System for Thermal Detection

Minsoo Kang(강 민 수 姜 敏 洙)

Department of Information and Communication Engineering

DGIST

2021

Artificial Tactile Sensor based on Pressure & Temperature Hybrid Sensing System for Thermal Detection

Advisor: Professor Jae Eun Jang
Co-advisor: Professor HongKi Kang

by

Minsoo Kang
Department of Information and Communication Engineering
DGIST

A thesis submitted to the faculty of DGIST in partial fulfillment of the requirements for the degree of Master of Science in the Department of Energy Science & Engineering. The study was conducted in accordance with Code of Research Ethics[1]

11. 23. 2020

Approved by

Professor Jae Eun Jang (signature)
(Advisor)

Professor Hongki Kang (signature)
(Co-Advisor)

[1] Declaration of Ethical Conduct in Research: I, as a graduate student of DGIST, hereby declare that I have not committed any acts that may damage the credibility of my research. These include, but are not limited to: falsification, thesis written by someone else, distortion of research findings or plagiarism. I affirm that my thesis contains honest conclusions based on my own careful research under the guidance of my thesis advisor.

Artificial Tactile Sensor based on Pressure & Temperature Hybrid Sensing System for Thermal Detection

Minsoo Kang

Accepted in partial fulfillment of the requirements for the degree of Master of Science.

11. 23. 2020

Head of Committee Prof. Jae Eun Jang (signature)

Committee Member Prof. Hongki Kang (signature)

Committee Member Prof. Hyuk-Jun Kwon (signature)

MS/IC
201922001

강 민 수. Minsoo Kang. Artificial Tactile Sensor based on Pressure & Temperature Hybrid Sensing System for Thermal Detection. Department of Information & Communication Engineering. 2021. 49p. Advisors Prof. Jae Eun Jang, Co-Advisors Prof. Hong Ki Kang

ABSTRACT

Artificial tactile sensors with various types of sensing mechanism have been developed in order to mimic the human's tactile sensations in nowadays. Among many input parameters which provide useful information about skin state, especially, sensations of temperature and pressure are the most important tactile factors, because these can be used to generate advanced tactile sensation such as pain, vibration, hardness. Therefore, these two senses are the important mimic points of artificial skin technology, for realization of an artificial tactile system. we should consider mechanisms to detect these two parameters, temperature and pressure, and a systematic integration. To measure these external stimuli, data acquisition with connecting wire between the sensor and the signal processor are required. However, when integrating numerous amount of various unit sensors, the same number of wires as elements are required. As a result, numerous wire connections cause the limitation of designing sensors with complexity of the sensor structure.

In this paper, the design of temperature sensor was simplified utilizing a single resistor placed on top layer of the hybrid sensor system and the method was studied to enhance sensitivity of thermal detection the same as one of the multi-thermal sensor array design. To measure exact the temperature value of object, which is smaller than the size of sensor, the signal processes was developed by capturing maximum slope of the resistance variation on a single resistive sensor and utilizing the area information which is acquired from micro sized pressure sensor arrays positioned under the temperature sensor. Slope provides information related to total thermal energy and a more precise temperature value was calculated utilizing an area information on pressure sensor arrays. As a result, the hybrid tactile sensor detected successfully the temperature levels from various dimensional contact stimuli with under 300msec response time as well as different pressure levels and the shape of objects.

Keywords: Piezoelectric pressure sensor, resistive temperature sensor, artificial tactile sensor, multi-sensing

List of Contents

III. EXPERIMENTAL DETAILS

IV. RESULTS AND DISCUSSION

List of Figures

I. INTRODUCTION

1.1 Overview

Imitation of five types human sensation such as sight, hearing, smell, taste, tactile with engineering method is interesting area for researchers nowadays including the past. Inventions such as television, camera, audio, telephone have been studied from the past to mimic vision and hearing. In nowadays, a lot of efforts are being made to mimic a various types of senses, such as taste, touch, smell for applying to many applications. However, the researches remain relatively more to be done on mimicking tactile receptors. In the sense of touch, mechanoreceptors, thermoreceptors, and nociceptors generate action potentials due to external stimuli, and interact with the human nervous system[1]. The appropriate integration of these receptor signals produces a variety of psychological sensations, including hardness, vibration, pain, warmth, and cold. These tactile sensations can be implemented with the most basic senses, temperature and pressure variables, and follow the most basic principle that mimics the receptors distributed in human skin. By applying these tactile parameters, research is being conducted in the field of robotics, biomedical devices, or human/machine interfaces[2]. To mimic those two kinds of tactile sensation by utilizing engineering approaches, many methods have been proposed to employing which mechanisms should be employed at the sensor. For example, piezoelectric[3][4][5], triboelectric[6][7][8], capacitive[9][10], and resistive[11][12][13] mechanisms are used to mimic the mechanical receptors responsible for pressure sensation. In addition, research is being conducted with pyroelectric[14][15], Seebeck effect[16][17], and resistive[18][19][20] methods to mimic the thermoreceptor responsible for temperature. In addition, efforts are being made to mimic nociceptors that can be prevented from external stimuli by detecting high pressure and overheating[4][16]. In order to implement these mechanisms, it is necessary to select an appropriate material for composing the device and design the structure. Moreover, it is possible to mimic the ideal human skin that embodies different sensations by integrating various kinds of sensors into a single

electronic device. For this, sensors simultaneously detect signals from multiple external stimuli and provide useful information on robotics or humans. However, the more various types of sensors that are combined, the more complex electronic devices become. For example, each sensor that detects different variables generates an unintended output from a single stimulus, which called decoupling[21][22]. Also, as the number of sensors increases from combination and miniaturization, the number of wire connections between the signal receivers and generators increases and it results complication[23]. In order to solve this problem, a design of multiplex strategy is required, but there are limits of stretchable substrates[24]. It is necessary to present the possibility of implementing the simplified design in case the sensor's structure is complicated by multiple sensing system.

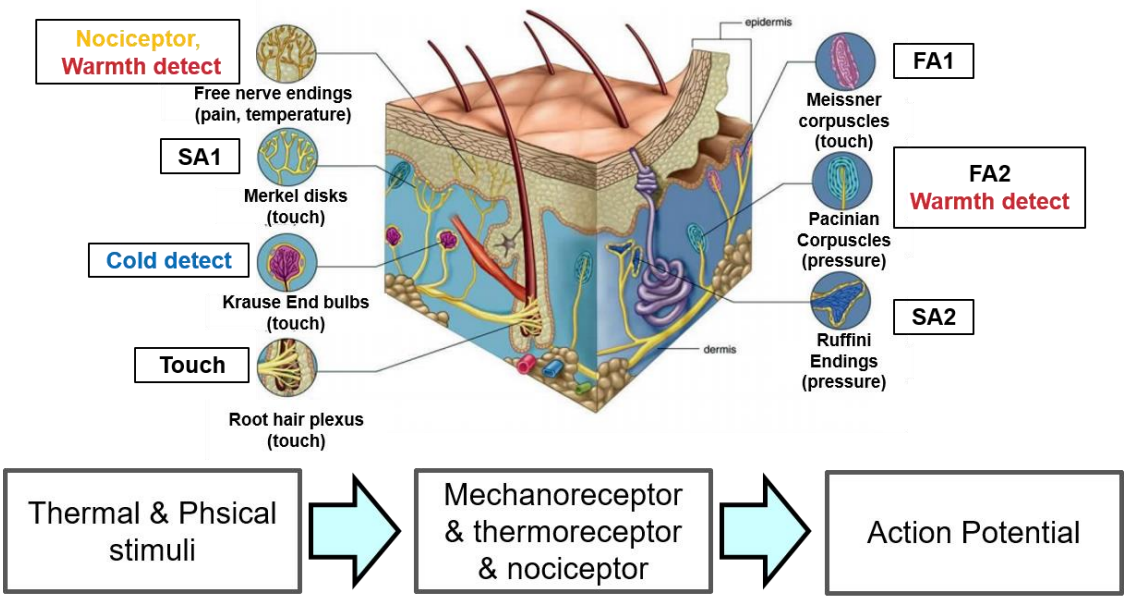

Fig 1.1.1 schematic of tactile receptors and process of sensing[50]. Tactile receptors generate action potential due to external stimuli

1.2 Motivation

This study will focus on implementing pressure and temperature sensation simultaneously. Based on the most two basic human tactile senses, it is applied to robotics to realize the ability to sense the sense of touch by various external stimuli. In the case of human finger skin, a relatively large number of pressure receptors is distributed compared to receptors of

temperature sensation[25][26]. To motivate this, it mimics human finger sensations by placing a large number of pressure cells and a small amount of temperature sensors. This allows the pressure sensation to have a relatively large resolution, allowing for sensitive detection of physical stimuli. However, although the resolution of the receptor for thermal stimulation is relatively low, humans do not have a big problem in detecting the temperature of an object. If these characteristics are applied to robotics, there will be no obstacles in distinguishing the temperature in general, but there is a possibility, that accurate values cannot be recognized in distinguishing the temperature level from a narrow object. If overheating is irritated, it may cause damage to the robotics prosthesis. There is a method of using temperature sensors as many as the number of pressure sensors placed, but the structure becomes complicated due to the increase of the signal generator and receiver. This increases the output signal to be read, requiring more wire connection and reaching the limit of sophisticated fabrication processes, making cost problem[28]. To improve this, this paper focuses on simplifying the structure of the multi-sensing sensor and maximizing its function.

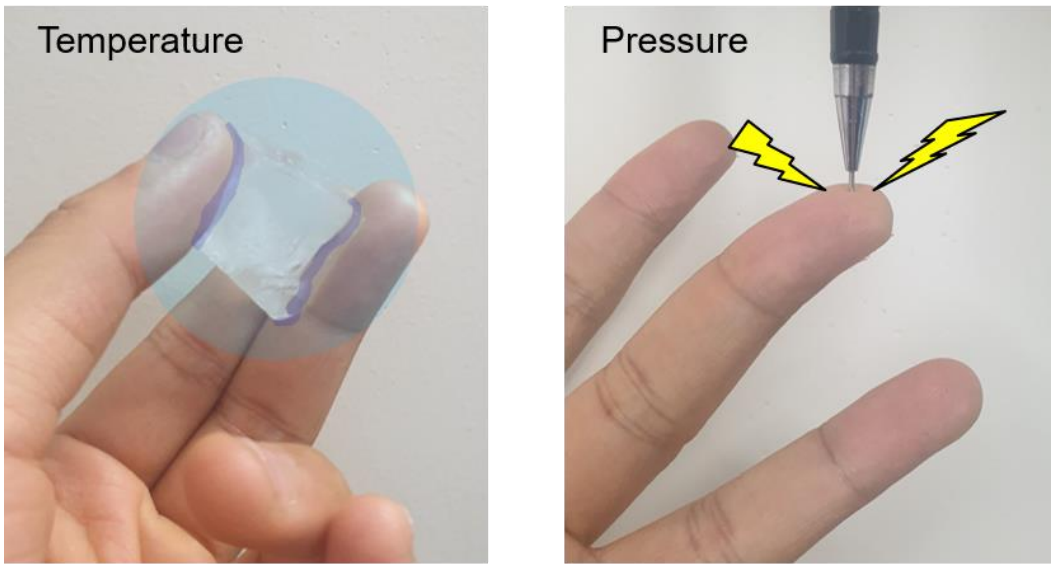

Fig 1.2.1 Images of stimuli temperature and pressure. The human can feel two basic tactile sensation at the fingertips. (a) The temperature which includes warmth and cold. (b) touch sense can be made by pressure stimuli

This thesis shows about a simplified multi-sensing sensor with the following sequences: in Chapter 2, we will talk about the human tactile sensing system to understand about the basic information about receptors on the skin, and take a look for the previous works of temperature and pressure sensor. The device concepts which include the structure, Fabrication process, experimental setup will be introduced in Chapter 3. Solving the unintended issues caused by the simplified structural design and utilizing the characteristic will be demonstrated in Chapter 4. Chapter 5 concludes the thesis by presenting the conclusion of the thesis, contents to be resolved in the future, and the possibility of application of the technology.

Ⅱ. BACKGROUNDS

2.1 Human tactile system

In order to realize tactile imitation, it is necessary to understand the human tactile system. Based on this, various types of sensor mechanisms can be implemented to help properly mimic receptors. Chapter 2 introduces the human tactile system and previous work.

2.1.1 Tactile receptors

The sense of touch is involved in somatosensory sense, which is a complex system of neurons and nerve pathways. Tactile receptors distributed among the skin respond to external stimuli and activate action potentials. These signals are transmitted to the brain along neural pathways, where humans feel the sensations transmitted from the skin[29]. Tactile receptors that convert external stimuli into appropriate signals are classified into mechanoreceptors, thermoreceptors, and nociceptors[30]. Mechanoreceptors mainly convert the sense of external pressure to signals and are broadly classified into 2 types: slow adaptive receptors (SA-I: Merkel cells, SA-II: Ruffini endings) and fast adapting receptors (FA-I: Meissner corpuscles, FA-II: Pacinian's corpuscles). The slow adapting receptors sensitively respond to static pressure, while fast adapting receptors preferentially respond to dynamic pressures or vibrations[7]. Detailed classification of the 4 types reveals a clear role for each receptor. Merkel cells(SA-I) are positioned near the surface of the skin and measure static force with a high resolution by high density of the receptors. Ruffini endings(SA-II) are placed relatively deeper and less sensitive due to their low density but can detect stretches of the skin. Meissner corpuscles(FA-I) are positioned near the surface of the skin and measure dynamic pressures with a high resolution by high density of the receptors. Pacinian's corpuscles(FA-II) are placed in relatively deeper with low density and have strength on detecting high frequency of vibration[1]. Thermoreceptors which contain warmth and cold have a relatively lower density distribution compared to pressure receptors. Among the receptors in human skin, Free

nerve endings, Ruffini endings sense warmth and Krause end bulbs sense cold. Cold spots have a density of 6~23 (average 12~13) per cm^2 with the responding range of 17°C ~27°C. Hot spots have relatively small amounts about up to 3 per cm^2 with the range of response, 30°C ~45°C[31]. Nociceptors react when excessive stimuli (pressure, heat, cold) are applied. Nociceptors react when exposed to excessive pressure, heat and cold stimuli, and can mitigate threats from the external environment. In terms of temperature stimulus, the range in which humans purely sense only temperature is between 15°C and 45°C, and when outside this range, it causes pain by activating the nociceptor from strong cold and overheating[32].

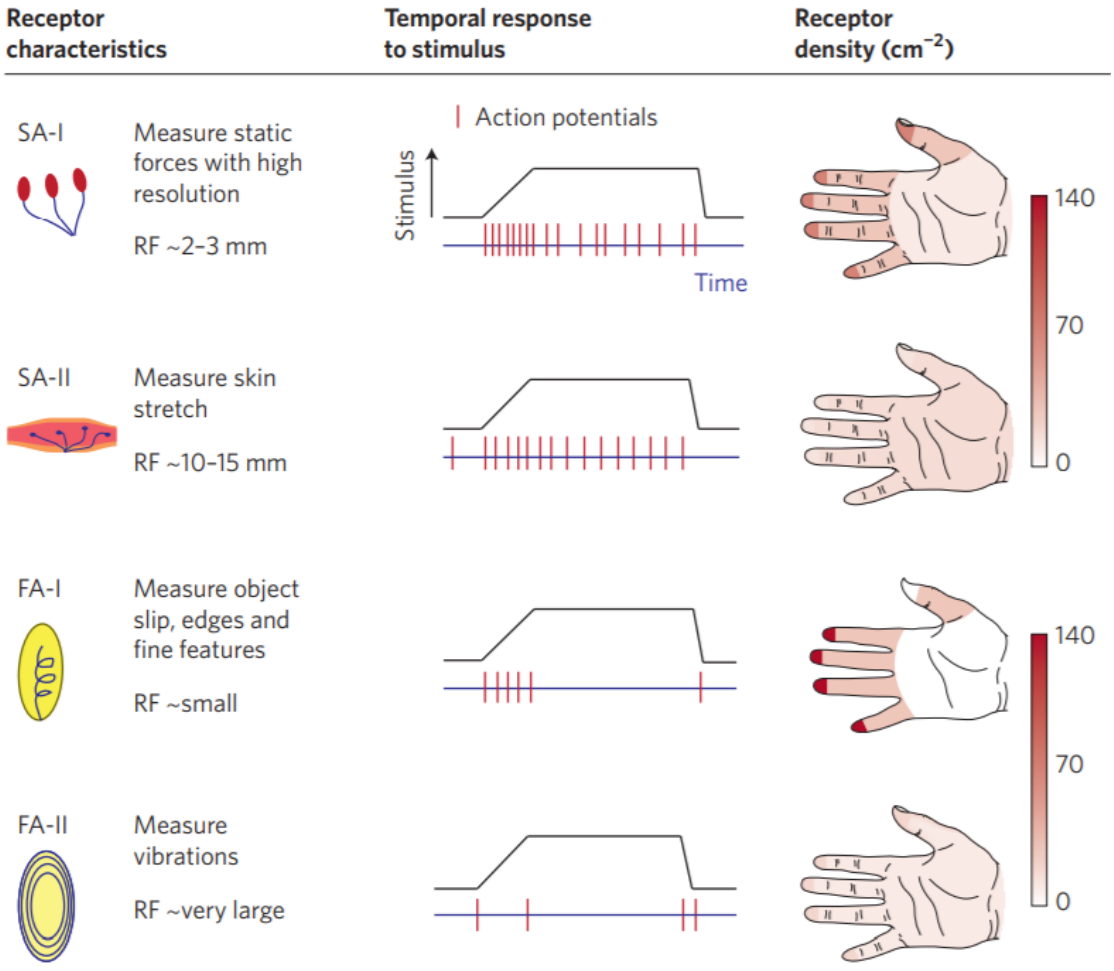

Fig 2.1.1.1 Information of Receptors characteristics and density[1]. Markl cells(SA-I), Ruffini receptors(SA-II), Meissner corpuscles(FA-I), and Pacinian corpuscles(FA-II) are typical mechanoreceptors. Each receptors has there specific characteristics and densities.

2.2 Previous Works

Research is being conducted to implement multiple sensing by arranging multiple sensors that can accept various stimuli to realize human tactile sensation[33]. Resistance, thermoelectric, and pyroelectric have been studied to mimic temperature sensing, and resistance, electrostatic, triboelectric, and piezoelectric methods have been used to detect pressure. In order to implement each sensor, we consider the appropriate material and proceed with the design. By integrating the two senses, temperature and pressure, it realizes a variety of senses and can be applied to many different applications. However, problems such as cost penalties and decoupling are occurring due to complex structures. Therefore, in order to integrate multiple sensors into a single system, it is necessary to simplify the structure.

2.2.1 Pressure Sensing Mechanism

Pressure is a parameter that mimics mechanoreceptors and is the most important sense in designing static or dynamic physical stimuli. It is one of the most common imitations when it comes to imitating the sense of touch. Several pressure sensors currently under study are described.

2.2.1.1 Piezoelectric Sensor

In the case of a piezoelectric sensor, it generates a voltage signal by automatically generating energy by an external force[2]. To produce the piezoelectric effect, various materials such as zinc oxide nanowire (ZnO NW), lead zirconate titanate(PZT), Polyvinylidene fluoride(PVDF) are used, and it is selected by considering whether it is possible to be flexible or proper materials. Due to its fast response speed and high sensitivity, it is often used to measure vibrations, and is used in dynamically acting applications such as slip rather than static signals. Shin at al.[34] proposed a tactile sensor utilizing a piezoelectric array structure. A high-resolution shape was detected by outputting the voltage peak with a fast response speed. A piezoelectric element that is advantageous for dynamic stimulation is used to detect surface sliding motion. Also, Jeong at al.[4] Propose tactile sensor that detects pain using the high

sensitivity of piezoelectric sensors. Using 9 multi-cell structures, it detects light touch and strong pricks. A psychological tactile sensor was fabricated by designating a certain level in consideration of the ambient voltage.

2.2.1.2 Capacitive Sensor

Capacitive sensors are used in applications using several principles. There is a method of implementing on-off by changing the capacitance value by creating a parasitic capacitor due to external stimuli, and this is mainly applied to display field[18]. Alternatively, one of the methods applied in the robotics field is to detect a sensitive reaction by changing the gap size of the capacitor by external pressure. It has the advantages of high sensitivity, better frequency response, and less decoupling from temperature[35]. But has the disadvantage of noise issues due to the sensitivity from parasitic capacitance. Wan at al.[36] Proposed a sensor that measures pressure by changing the gap between two capacitor plates. A micro tower is formed on the surface of polydimethylsiloxane(PDMS) to form a capacitive pressure sensor with high sensitivity and response time. Due to the stretchability characteristics of PDMS, silver nanowire (AgNW) was used as an electrode. Maiolino et al.[37] Shows an example of applying a capacitive sensor to a robot. It has high sensitivity and resolution from external pressure by using a 3D fabric that can deform the dielectric layer of the capacitor.

2.2.1.3 Triboelectric Sensor

The triboelectric effect appears when the material in contact is subjected to friction due to touch, shear friction due to sliding motion, or twist. When rubbing two different materials, the surface charge is induced and becomes polar[38]. This characteristic is used for energy harvesting or signal sensing. Chun et al.[7] proposed a sensitive triboelectric generating structure by laminating roughly shaped PDMS on the surface. It detects vibrations slipping on the surface and detects the roughness of the surface by mimicking the fast adaptation receptor. 12 types of fabric's surfaces were successfully identified using deep learning. Wu et al.[39]

proposed a study to induce triboelectricity using PI:rGO film and Al film. It mimics the part of human memory by trapping electrons in a body trap placed on the PI:rGO film.

2.2.1.4 Piezoresistive Sensor

Piezoresistive sensors convert force changes into resistance changes, which can be easily detected by electrical measurement systems. It changes the conductivity while changing the structure of the sensor. It has been widely used due to its simple design and measurement mechanism of resistance values[40]. It has the advantage of high sensitivity and wide measuring range but has the disadvantage of being affected by hysteresis effect and temperature. Wang et al.[11] Proposed a sensor that measures external pressure by overlapping two substrates on which graphitic nanocarbons are deposited. Due to the external pressure, the contact area between graphitic nanocarbons increases, and the conductivity increases and at the same time triggers tunneling conduction. We studied a high-sensitivity electronic skin that can measure pressure stably even on stretchable substrates. Kim et al.[23] Proposed a pressure sensor which was deposited with metal or semiconductor in the shape of a serpentine-shaped electrode. These sensors can measure external pressure without the need for complex material processing.

2.2.2 Temperature sensing mechanism

Temperature sensors are under study to mimic a thermoreceptor that humans can detect warmth and cold. These parameters are required for tactile sensors, including biosensors and human/machine interfaces.

2.2.2.1 Pyroelectric Sensor

pyroelectricity refers to the electrical polarization of a specific substance to generate a voltage in response to an applied temperature change. By converting thermal energy into electricity, it is able to create a self-powered temperature sensor that automatically detects temperature

changes without additional batteries[2]. Graz et al.[41] proposed a pyroelectric temperature sensor by making a composition of piezoelectric polymer and ceramic particles. In order to induce high polarization, the polling procedure was carried out by heating to 120°C degrees and applying voltage. A cell matrix structure is realized by combining a material that represents pyroelectric and creates a piezoelectric effect on TFT. Tien et al.[42] proposed a temperature sensor by applying P(VDF-TrFE) material to the gate insulator layer in the OTFT(Organic Thin Film Transistor) structures. The conductivity is changed by inducing polarization by pyroelectric effect due to external temperature stimulation.

2.2.2.2 Thermoelectric Sensor

The thermoelectric device is based on the seebeck effect, which utilizes the temperature difference across the device to induce the diffusion of charge carriers. It has an advantage in terms of energy efficiency because it generates a self-powered effect, but it has the disadvantage that absolute temperature measurement is impossible. Sim et al.[16] proposes a method of simultaneously implementing the piezoelectric effect and the seebeck effect using zinc oxide nanowire. They employed the material with doped semiconductor properties that senses temperature by generating current due to diffusion of free electron charge carriers.

2.2.2.3 Resistive Temperature Sensor

Resistive temperature detectors work based on the change in the electrical resistance of a metal with temperature. This lies in temperature accuracy and reproducibility. There are two types of temperature coefficients. It is classified into a negative temperature coefficient(NTC) that decreases the resistance values as the temperature increases, and a positive temperature coefficient(PTC) that decreases the resistance value when the temperature increases. The properties differ depending on the material used. Dankoco et al.[43] fabricated a temperature sensor using a simple inkjet printing technique. A silver nanoparticle solution was extracted from the nozzle to form a pattern. Shin et al.[44] reported a temperature sensor incorporating a metal and metal oxide into a monolithic structure. By irradiating a laser on the substrate

coated with NiO nanoparticles, Ni metal is produced through a reduction phenomenon. NiO is designed as a temperature sensor with NTC coefficient, which is highly reactive to temperature between two metals.

2.2.3 Multi Sensor

The multi-sensing sensor is a necessary part to fully imitate human skin. It can be applied to various applications by mimicking the temperature, pressure and pain receptors distributed in people's skin. However, in this imitation process, numerous sensors are required. Also, there are difficulties in decoupling and complex structure design caused by collecting various types of information. Zhao et al.[45] presented a multifunctional electronic skin that detects temperature and pressure stimuli, distinguishes material types, and detects wind. It is a flexible platinum (Pt) film that is used to detect the ambient temperature. The heated metal detects the wind using the convective heat flux caused by the wind. It also detects pressure using the change in thermal conductivity changed by pressure. Hua et al.[46] proposes a multi-sensor that can detect temperature, strain, and pressure, including a capacitive humidity sensor. We have developed an electronic skin that can realize multi-functionality according to the type of design using metal electrodes.

2.3 Principle of Piezoelectricity

Piezoelectric effects occurs from linear electromechanical interactions between mechanical and electrical states in crystalline materials that do not have inverse symmetry[47]. The piezoelectric effect is related to the principle that an electric dipole moment occurs in a solid. The piezoelectric material forming the crystal is electrically neutral as particles with positive charges and particles with negative charges are regularly arranged. In addition, the positions of positively charged particles and negatively charged particles in the crystal are shifted, so that one side is positive and the other is negative. The formula of the piezoelectricity phenomenon that results the voltage level is defined as

$$V = \frac{dLF}{\varepsilon_0 \varepsilon_r A} \tag{3.1}$$

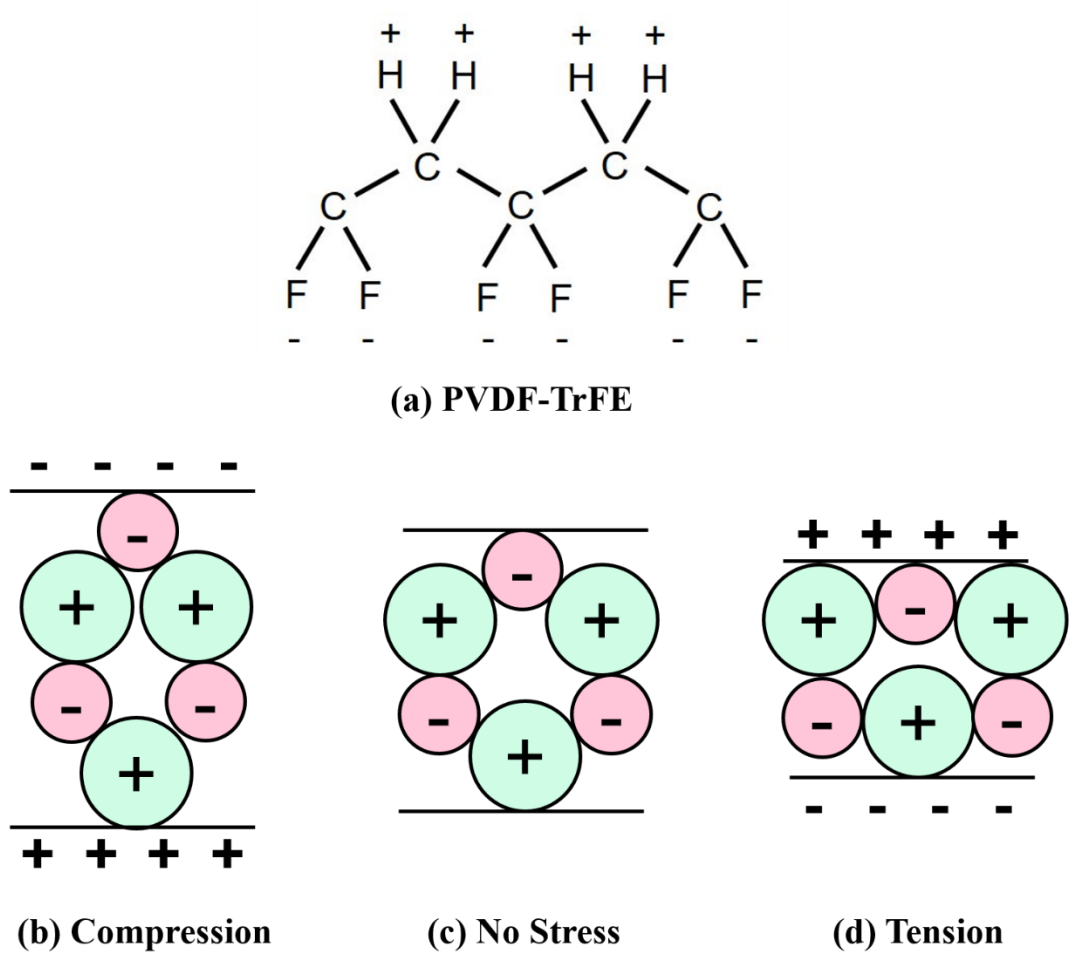

Fig 2.3.1 Principle of the piezoelectric effect of PVDF-TrFE. (a) PVDF-TrFE is the piezoelectric material which is located the positive charge and negative charge on direction of each side respectively. (c) is the steady state of the piezoelectric material. (b) When a compressional force is induced, the polarization charges covered the surface of the material. (d) When a strain is applied to the material, the polarization charge is the opposite from that of (a).

where L, $F, d, \varepsilon_0, \varepsilon_r$ are the length, piezoelectric coefficient, force, absolute permittivity, dielectric constant of piezoelectric material, respectively. As shown in equation (3.1), the higher the applied force, the smaller the surface area (i.e. the higher the pressure), and the higher the thickness, the higher the voltage is generated. Fig. 2.3 explains the structure of the piezoelectric material PVDF-TrFE and the principle of generating piezoelectric electricity by

external stimulation. The shape of the material is deformed by the action of compression and tension, and the polarization of the instantaneous charge is expressed due to polarization.

2.4 Principle of Resistive Temperature Sensor

A resistive temperature sensor is an electrical device that uses the property of changing the resistance of a material according to temperature. The drift velocity, which is the speed at that an electric charge moves through the field, is proportional to its mobility. However, as the amount of heat energy increases, the degree of lattice scattering increases, which causes the atoms to vibrate a lot and collide with moving electric charges. Eventually, the electron mobility decreases and the electrical conductivity decreases. Thermal stimulation of the device can be detected through the change in electrical conductivity caused by such heat, and the temperature sensor is used by assuming a linear relationship between temperature and conductivity. Fig 2.4 shows the schematic of lattice scattering phenomenon that effects the movement of electrons. Electron mean free path will be reduced when the temperature increase, because of the low mean free path which causes the low conductivity.

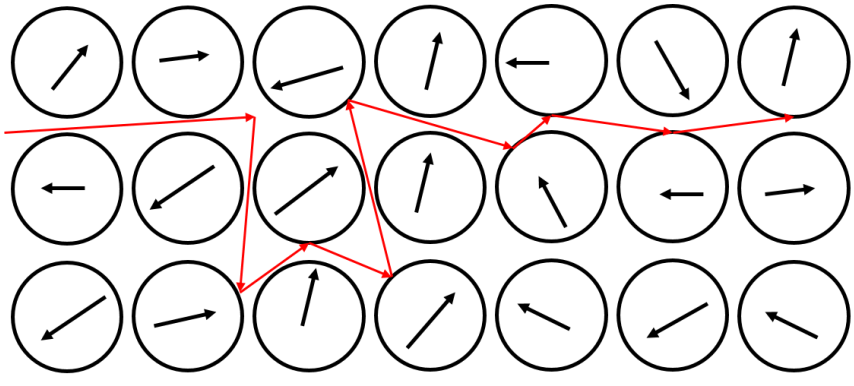

LATTICE SCATTERING

$$\text{Mean free path} \propto \frac{1}{Temperature} \propto \frac{1}{Resistance}$$

Fig 2.4.1 Principle of the resistive temperature sensor. Due to the lattice scattering effect, conductivity changes when the temperature has been induced at the sensor

Ⅲ. EXPERIMENTAL DETAILS

3.1 Device Structure

The hybrid sensor consist of the top layer of the temperature sensor and the bottom layer of the pressure sensor. Fig 3.1.1 shows the overall structure of the hybrid sensor. The top layer

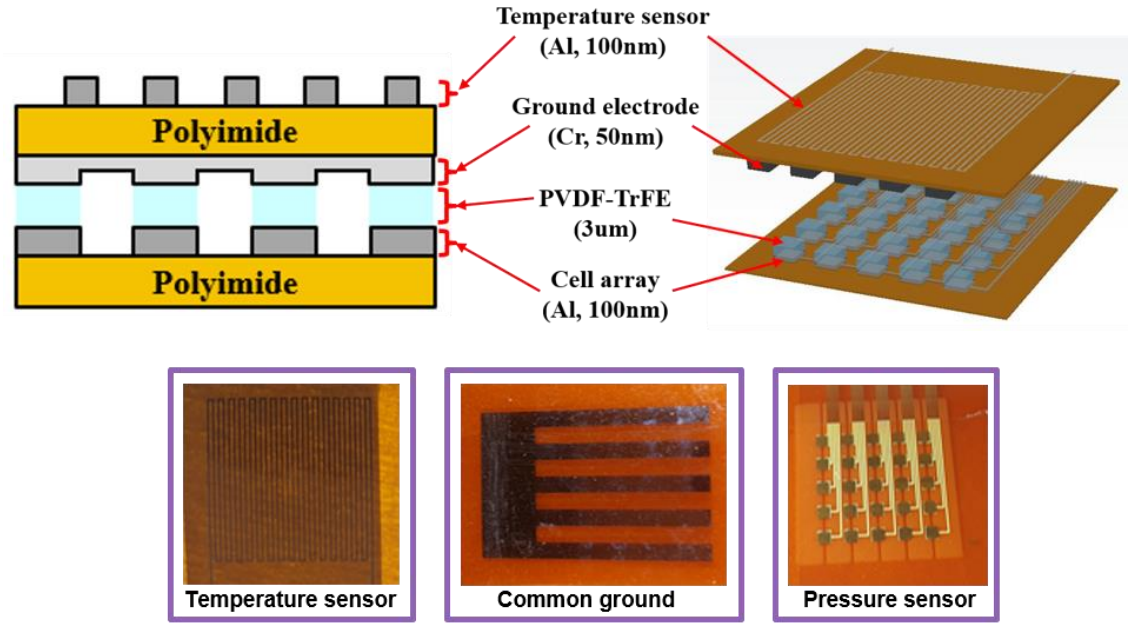

Fig 3.1.1 Schematic of hybrid sensor Structure. Hybrid sensor consists top and bottom layers which are overlapped together. Self-powered system are applied for pressure sensor and a simplified signle resistive temperature sensor is sensing the variation of resistance.

temperature sensor covers the whole area (0.9cm x 0.9cm) of the tactile sensor system and is deposited on a flexible polyimide substrate with a thickness of 100nm aluminum metal. The sensor is placed on the outer surface to be sensitive to the temperature caused by gastric stimulation. With a total of 32 curved patterns, the width is 0.1mm and the length is 30~40cm, which is relatively long compared to the width. The bottom layer is composed of an array of 25 piezoelectric cells and is composed of a square shape measuring 1mm in width and height. Piezoelectric materials are patterned for each cell array using PVDF-TrFE (polyvinyledenedifluoride-trifluoroethylene). In addition, pattern of the chromium metal(50nm) on the top layer where the metal is deposited on both sides are in direct contact with the

piezoelectric cells. This serves as a common ground electrode and stably emits a piezoelectric signal.

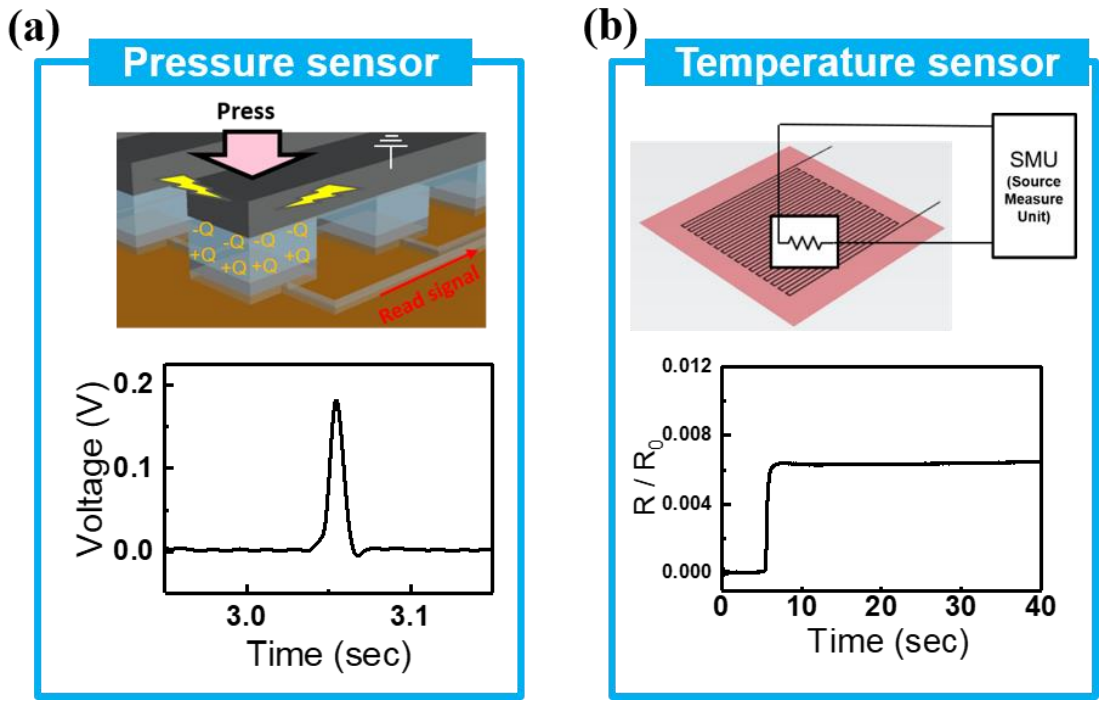

Fig 3.2.1 Schematic of working mechanism of each temperature and pressure sensor. (a) shows the piezoelectric effect which generates self-powered voltage energy. (b) shows the resistance variation from external temperature stimuli.

3.2 Device Concept

This hybrid sensor integrates the data of the temperature sensor and the data of the touch sensor to obtain the stimulated temperature level and area information. The temperature sensor derives an accurate temperature values by using the relationship between the resistance value and the temperature level using the temperature coefficient value of the material. Since the sensor derives temperatures below 60ºC degrees and above 20ºC degrees, it is assumed that the resistance value has a linear relationship with the temperature because of the small measurement gap. There is no difficulty in detecting the temperature when a stimulus is received in an area larger than the sensor area, but when a certain temperature iron or sharp material is touched, a narrow area is contacted and the detection limit of a single resistance

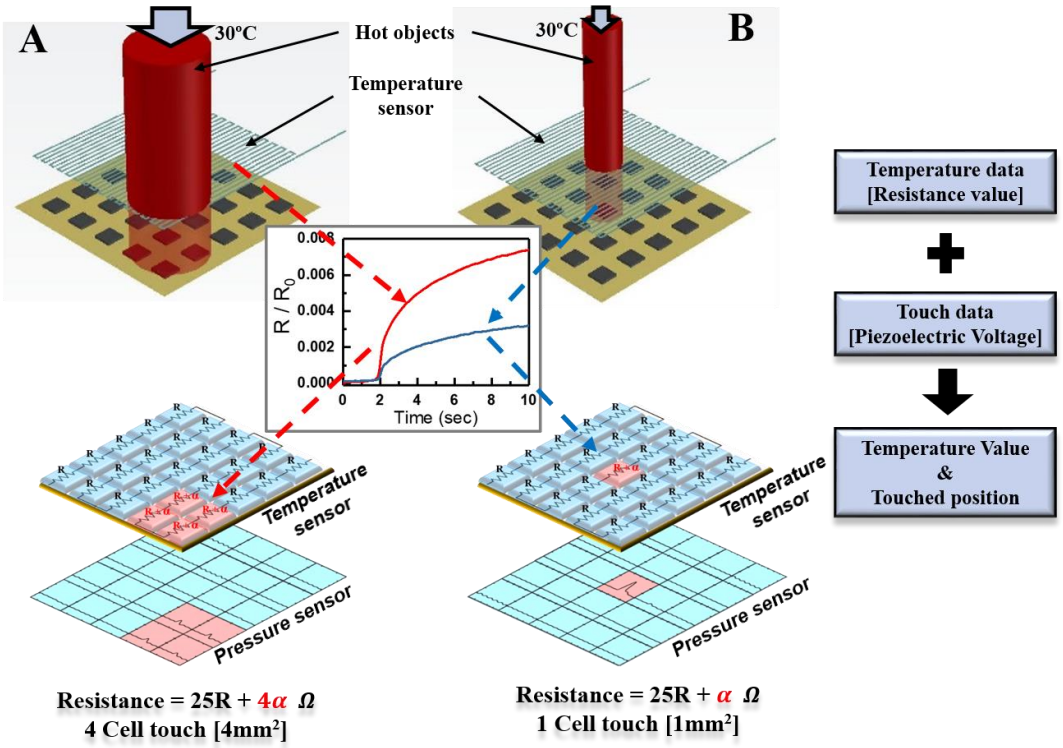

Fig 3.2.2 Hybrid sensor operation schematic detecting temperature & pressure. The resistance value detected by the resistive sensor is calibrated using the information of the pressure sensor to measure the correct temperature value.

temperature sensor appears. Area information is reinforced by using 25 piezoelectric sensors arranged on the bottom layer to detect these details. Although the temperature sensor has a series structure, it is assumed to be divided into 25 pieces and operated like each cell. Fig 3.2.1(a) shows schematic of the piezoelectric sensor used in the hybrid sensor. When pressure is applied to the cell, it generates an electrical signal, and a current along the electrode to detect the signal. Fig 3.2.1(b) shows schematic of detecting the changes of current value in real time by continuously applying DC power 5V.

Fig. 3.2.2 shows a schematic diagram of the sensor operating principle. Give. In the case of A and B, an object of 30ºC is in contact with the hybrid sensor, and the resistance values of the two temperature sensors change. Of the temperature sensors divided into 25 pieces, 4 in A and 1 in B are stimulated. In the case of A, the resistance values changes from the resistance value of 25R to 25R+4α, and in the case of B, the resistance value changes to 25R+ α,

resulting in a larger resistance change value of A. However, it is difficult to determine the exact temperature when this type of resistance change is detected. This is because the resistance value received from the SMU(source measure unit) system is different even though the same temperature is applied. This situation where different resistance values appears due to the same temperature and different contact areas can be solved by collecting and correcting area information with the pressure sensor part of the hybrid sensor. The resistance changed value(4α, α), additionally obtained by temperature, was expected to be proportional to the stimulated area, and the experiment was conducted from the viewpoint of deriving the correct temperature value by dividing by the collected area data.

3.3 Device Fabrication

Fig 3.3.1 shows the detailed process of the temperature sensor and pressure sensor. To fabricate a temperature sensor, organic matter and other particles are removed from the surface of a polyimide substrate for cleaning procedures. Negative type of the photoresist(PR) (AZ nlof-2035) was spin-coated on the cleaned polyimide substrate with 3000 revolutions per minute(RPM). After coating the PR, the coated substrate was baked on a hot plate in 105ºC for 1minute for PR adhesion and evaporating the solvent of the PR. The PR was exposed by ultraviolet ray (UV) with 70mJ/cm^2 through the photomask pattern. After exposure, The post exposure bake(PEB) procedure is carried out to diffuse the photo active compound(PAC) to smooth the surface of the PR. For that reason, the substrate was baked on the hot plate in 105ºC for 1minute. Then, the sample was developed by dipping in Az-developer for 2minute and rinsed by deionized(DI) water. The 50nm thick of chromium layer was deposited by using a magnetron sputtering system at DC input power of 100W, volume 40sccm of argon(Ar), pressure 5mTorr. After the deposition process, pattern of the common electrode was obtained through the lift-off process dipping in acetone and isopropyl(IPA) by ultrasonication. The patterned sample was flipped and for flatten the rough surface, scratched by previous photolithography process. The sample was spin coated with photosensitive polyimide(PSPI) (WPR-1201) with 2000 RPM. After coating the PSPI, the sample was baked on

a hot plate in 110ºC for 3min for adhesion and evaporating the solvent. The sample was baked on an oven in 190ºC about 1hours for curing. After curing, previous photolithography process was carried out for patterning the resistive temperature sensor with the conditions: PR spin-coated with 3000 RPM, soft baked 105ºC for 1min, exposure 70mJ/cm^2, PEB process in 105 ºC for 1min, develop process for 2min with AZ-300. The 100nm thick of aluminum layer was deposited by using a magnetron sputtering system with the conditions: DC input power of 100W, volume 40sccm of argon(Ar), pressure 5mTorr.

To fabricate a pressure sensor, similar process with fabrication of temperature sensor was carried out. 5x5 cell-array structure was fabricated on the polyimide substrate with the photolithography conditions: PR spin-coated with 2000 RPM, soft baked 105 ºC for 1min, exposure 70mJ/cm^2, PEB process in 105 ºC for 1min, develop process for 2min with AZ-300. Also deposition process was carried out with the conditions: The 100nm thick of aluminum layer was deposited by using a magnetron sputtering system with the conditions: DC input power of 100W, volume 40sccm of argon(Ar), pressure 5mTorr. After the lift-off process, PVDF-TrFE layer spin-coated on the 5x5 cell-array pattern for 3000RPM about 3~4 micro thickness. The sample was annealed at 130ºC for 2hours to change the phase-α to phase-β to achieve the piezoelectric properties[48]. After annealing process, reactive ion etching(RIE) process was conducted using shadow mask to individualize 25 cells and remove the polymer coated on the electrode of signal transmission line which stated in Fig 3.3.2(a). RIE condition carried out with input power 100W, oxygen volume 100sccm, pressure 10mTorr. Etching is performed for a total of 40 minutes, and a cooling process is conducted every 3 minute to prevent phase change due to heat. Fig 3.3.2(b) shows the etch-rate and over etched for remove the residual organic matters which causes small cross-talks. Fig 3.3.2(c) shows the optical images of the result of RIE process.

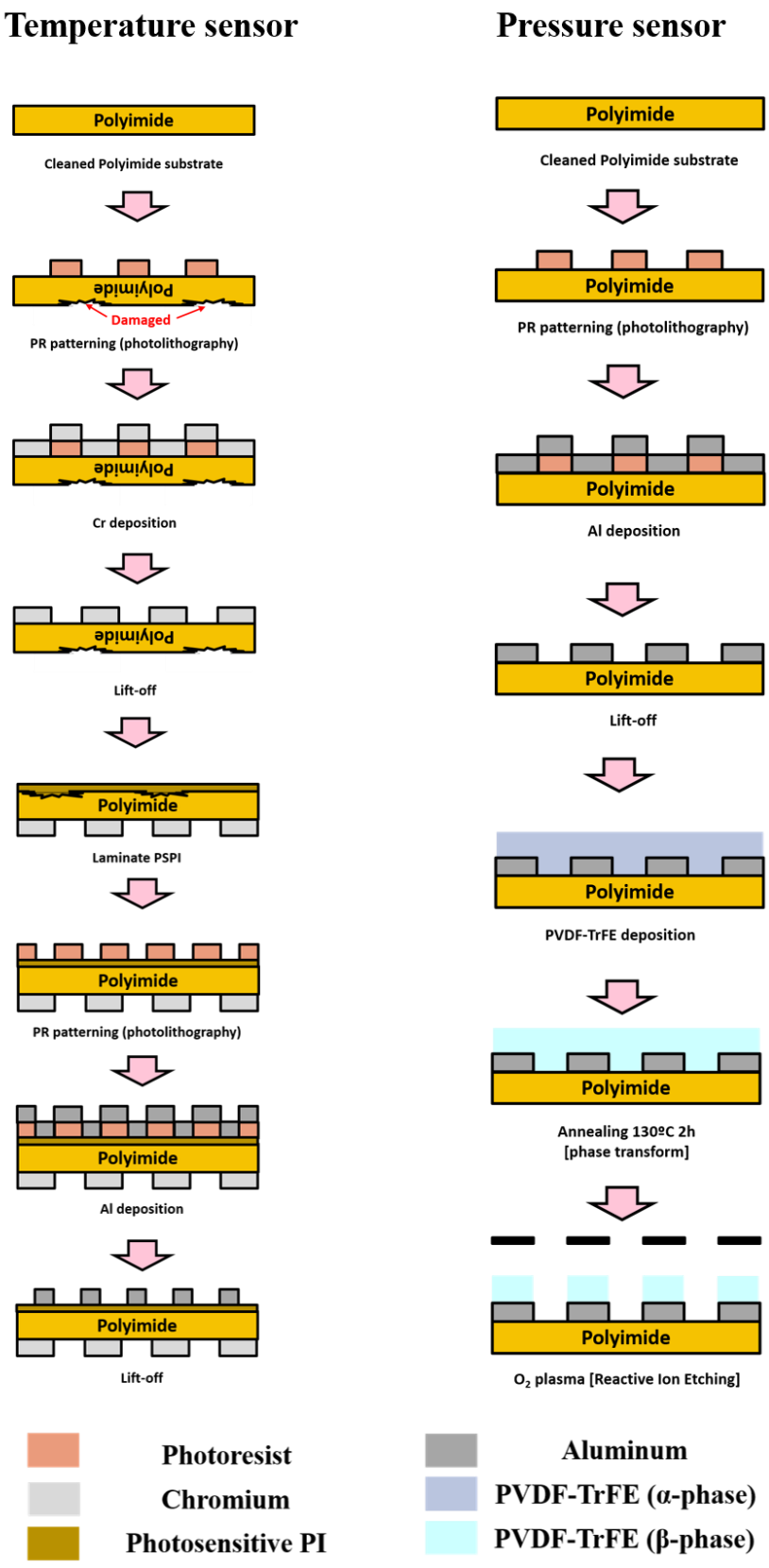

Fig 3.3.1 Fabrication process of temperature sensor and pressure sensor.

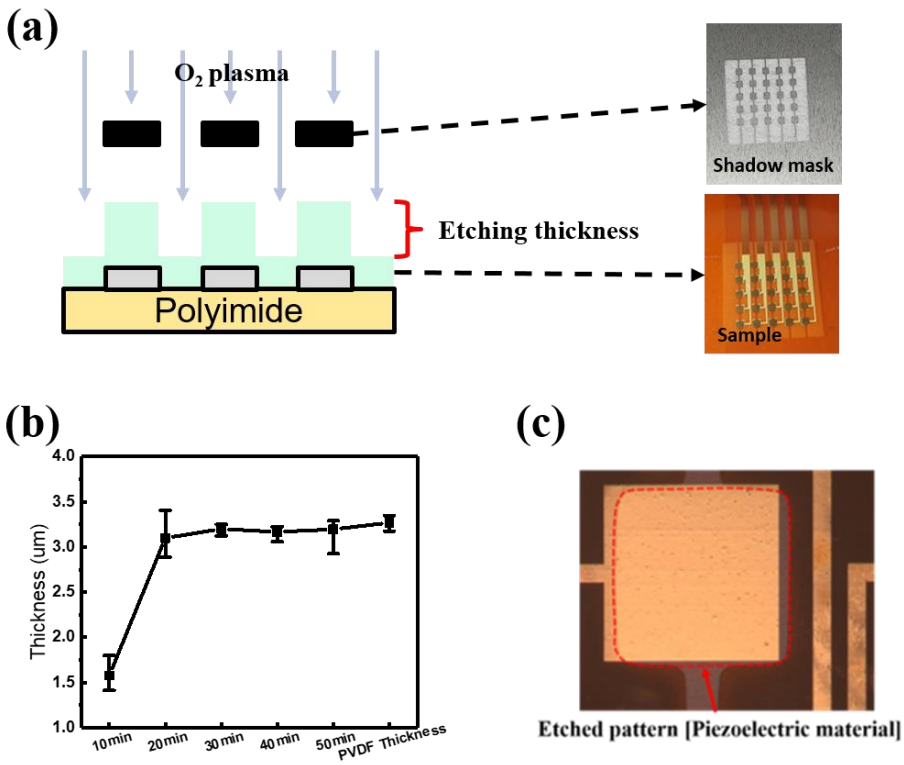

Fig 3.3.2 RIE process for patterning the piezoelectric material. (a) shows the schematic of the RIE process. O_2 plasma etching process was conducted with aligning the shadow mask on the sample. (b) Shows the time dependent etch rate of PVDF-TrFE. (c) Shows the optical images of etched pattern.

3.4 Experimental Setup

To measure a pressure heated with high temperature, we controlled the applied force using a linear stage(SM3-0806-3S, Science town) through the LabVIEW software which moves the axis of X, Y, Z. Each axis was controlled by using software program(PMC-1HS/PMC-2HS). To increase the temperature level of the contact object, we attach the tip on the peltier device and applied the constant DC power to the resistive temperature sensor with a power generator(GW Instek, GPS-3303). Combined tip with peliter device is covered with stylrofoam to prevent heat transfer to the sensor in the air. Pressure and temperature data received using DAQ and SMU respectively. All of the systems including DAQ, SMU, linear stage controller was interlocked with LabVIEW system.

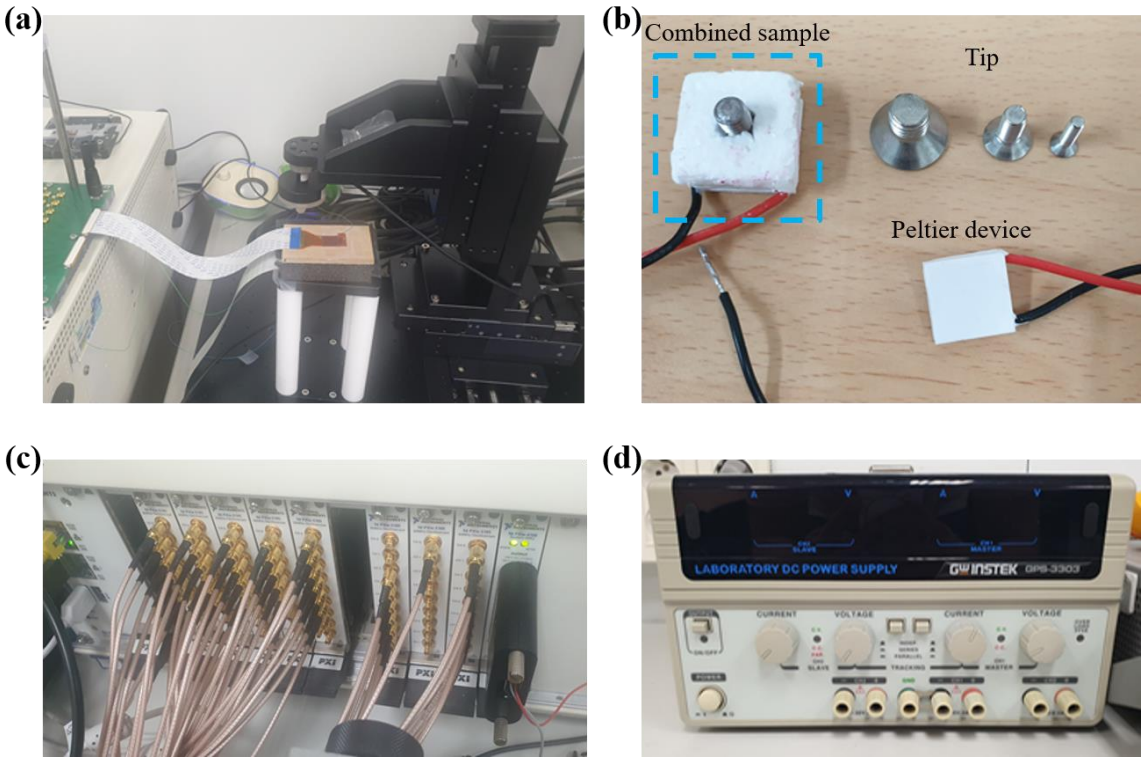

Fig 3.4.1 Measurement equipment for hybrid sensing system. (a) Optical images of linear stages, (b) tools for contact tip, (c) sockets of DAQ and SMU, (d) power generator for constant DC voltages.

Ⅳ. RESULTS AND DISCUSSION

4.1 Temperature Sensor Signal

Metal-based temperature sensors change their resistance value by external temperature. In Fig 4.1.1(a), the resistance value that varies with temperature is expressed as a formula. The resistance value is

$$R = R_0(1 + \alpha(T - T_0)) \quad (4.1)$$

where R_0, α_0, T, T_0 are the initial resistance value at 20ºC, temperature coefficient, induce temperature level, initial temperature level at 20ºC. In Fig 4.1.1(b), the temperature coefficient derived from the data is 0.001076. The slope of the change curve of the resistance value depends on the temperature coefficient value and determines the sensitivity of the sensor. The larger the temperature coefficient value, the greater the rate of change of the resistance value at the smaller temperature value. Fig 4.1.1(c) shows the resistance value that changes when a constant temperature(30ºC~60ºC) is applied to the sensor in the time domain. However, unlike when inducing a different temperature levels from the initial state in all areas of the sensor, it is difficult to obtain a constant resistance value in the time domain within a short time when a narrow contact surface is applied. First of all, a temperature sensor composed of a series circuit touches only a part of the resistance, so the performance cannot be fully realized. In addition, when hot or cold contact comes into contact with a part of the sensor, the temperature spreads to the surrounding area including the contacted part due to heat conduction. As time goes by, the ambient temperature of the contact point changes slowly and the resistance value is affected, so it cannot maintain a constant value. Even if heat is applied for a very long time, it has different results than applying temperature to the whole area of the sensor. Fig 4.1.2(a) shows a small area of thermal contact applied to the sensor. Fortunately, the tendency of the resistance value is different depending on the temperature change(25ºC~60ºC), and we have the possibility to distinguish the level. Fig 4.1.2(b) shows the temperature of 35ºC and applied to the sensor with tips with diameters of 2mm, 4mm,

and 7mm. Although contact was made under different contact area conditions, the tendency was clearly different according to temperature change. Considering the tendencies, there are two issues in which it is difficult to measure a clear temperature when measuring heat with a single resistance temperature sensor. First, it is difficult to receive a constant temperature value due to the very slow change in resistance. Fig. 4.1.3(a) shows the pressure applied to a small area and a total area respectively to the sensor with the same temperature of 35ºC. Unlike the schematic on the left, where the resistance curve saturates within a short period of time from the point when the heat contacts the sensor. the schematic on the right doesn't saturate even after 40 seconds. Also, it shows that the resistance change value is less than 30% comparing with the left case. If this type of detection result derived with introducing the formula of temperature resistance change, a big problem occurs in detecting the temperature sensation. Second, it is difficult to determine the size of the stimulated temperature because the amount of resistance change is different when a tip of the same temperature but different areas is applied to the sensor. Fig. 4.1.3(b) shows the change that occurred for 200 seconds in the time domain after applying a thermal contact of a different area to the sensor. Compared to the contact of the narrow area(diameter: 2mm), the contact of a large area(diameter: 7mm) causes a greater resistance change rate, and the final saturation value is also different. Also, it is difficult to see that the change in resistance is proportional to the area of the contact area because heat is spread from the contact surface due to heat conduction. To solve these two problems, we identify the tendencies and propose a solution.

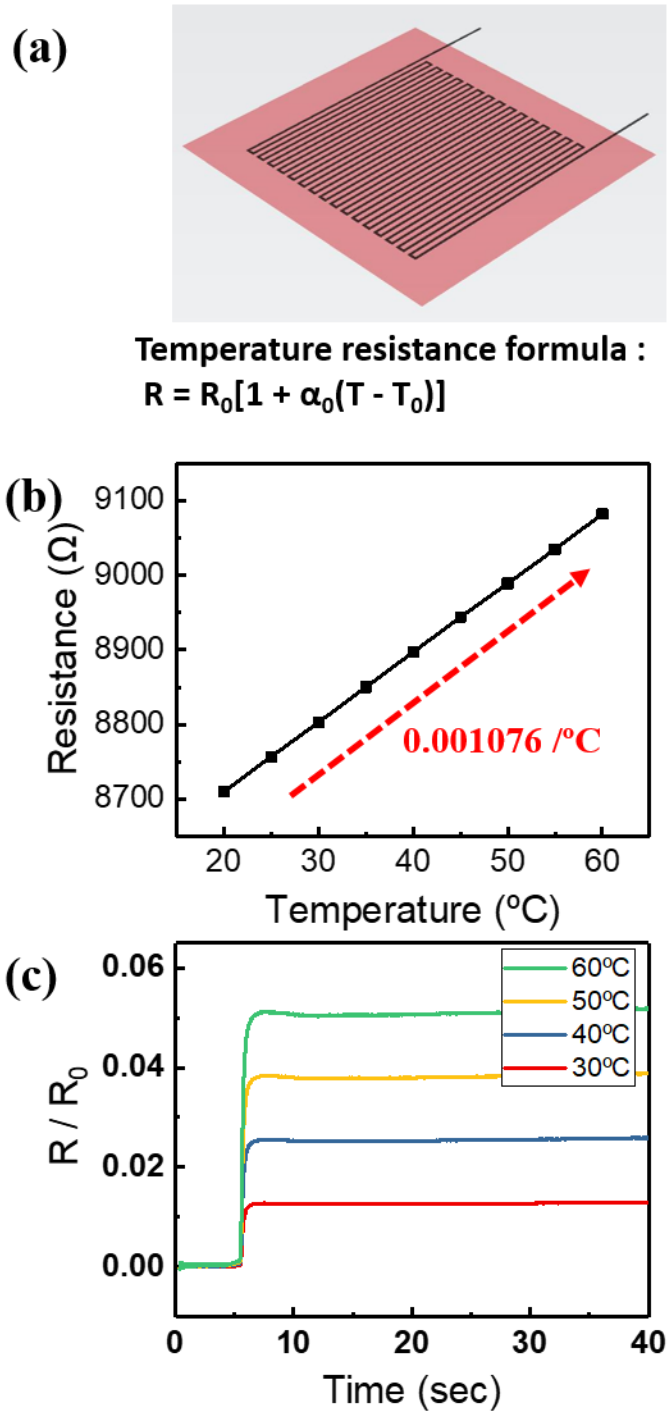

Fig 4.1.1 Characteristic of the resistive temperature sensor. (a) Schenatic of temperature sensor. (b) Temperature coefficient designat the variation curve of resistance. (c) Induced various temperature level cause different constant resistance level in the time domain.

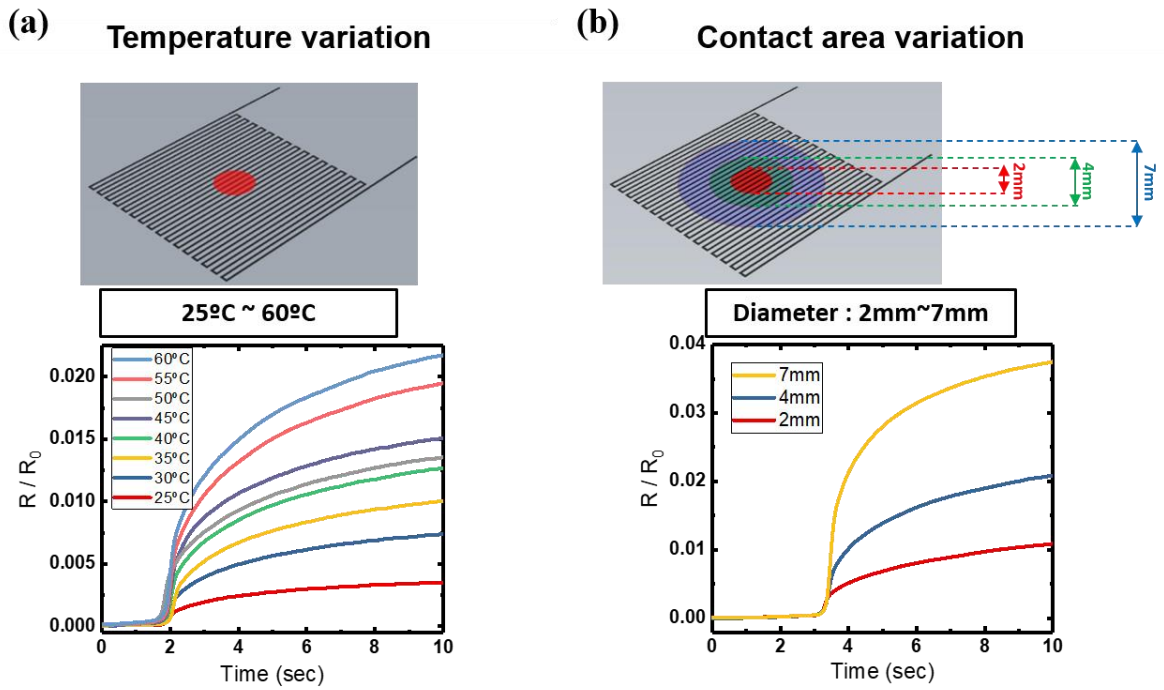

Fig 4.1.2 Schematics and results of partial contact on the sensor. (a) Resistance variation from contact of same area and different temperature on the sensor can be classified. (b) Resistance variation from contact of same temperature and different area on the sensor can be classified.

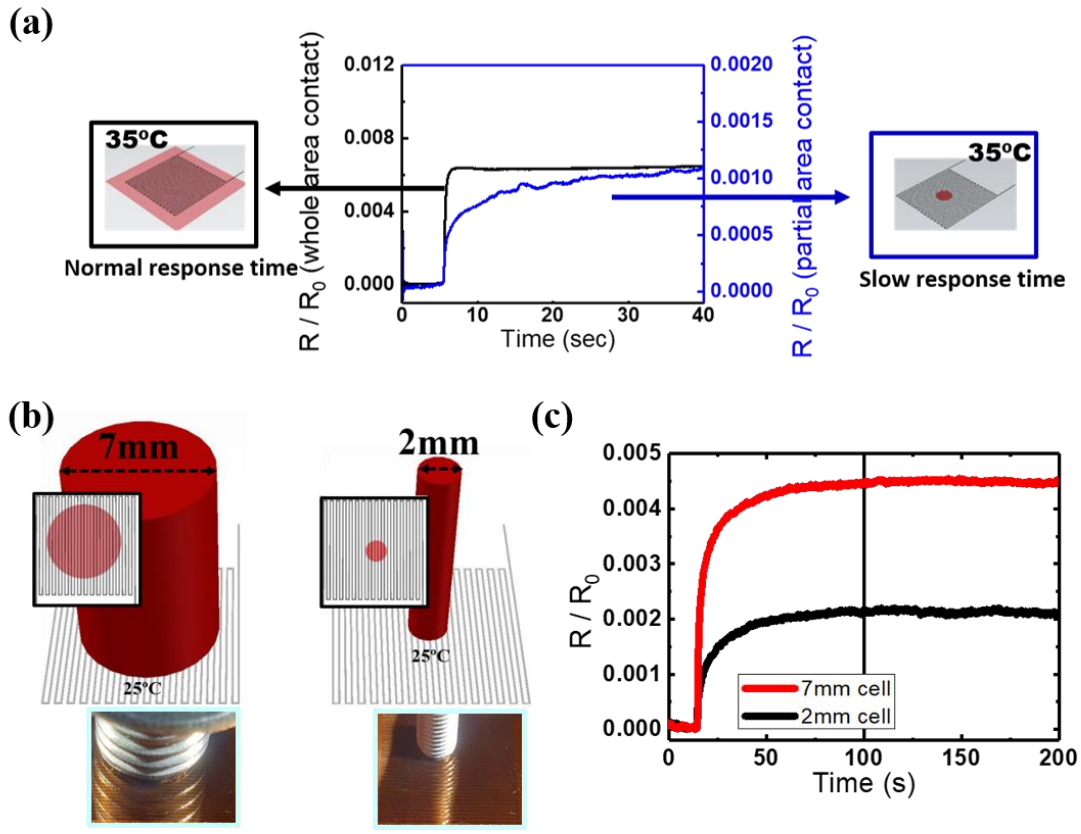

Fig 4.1.3 Issues of measuring the temperature with partial contact. (a) Very Slow response time of resistance variation (slow saturation). (b) Hard to classify same temperature if contact area is different.

4.1.1 Fast detection

In the conventional temperature sensing equation, the changed resistance value was detected based on the initial resistance value.

$$T = T_0 + \frac{R-R_0}{R_0} \cdot \frac{1}{\alpha} \qquad (4.1.1.1)$$

In order to solve the first problem of the slow resistance saturation rate, a clue was obtained from the information in Fig 4.1.2(a). Under normal circumstances, if the temperature is applied to the entire area of the sensor, it takes 1 to 3 seconds to saturate. However, when heat is applied to a small area, it takes more than 100 seconds to saturate, causing a problem. If you apply various temperatures to the sensor just before the temperature value is saturated,

you may find that the rate of change of resistance is different in time domain. Instead of using

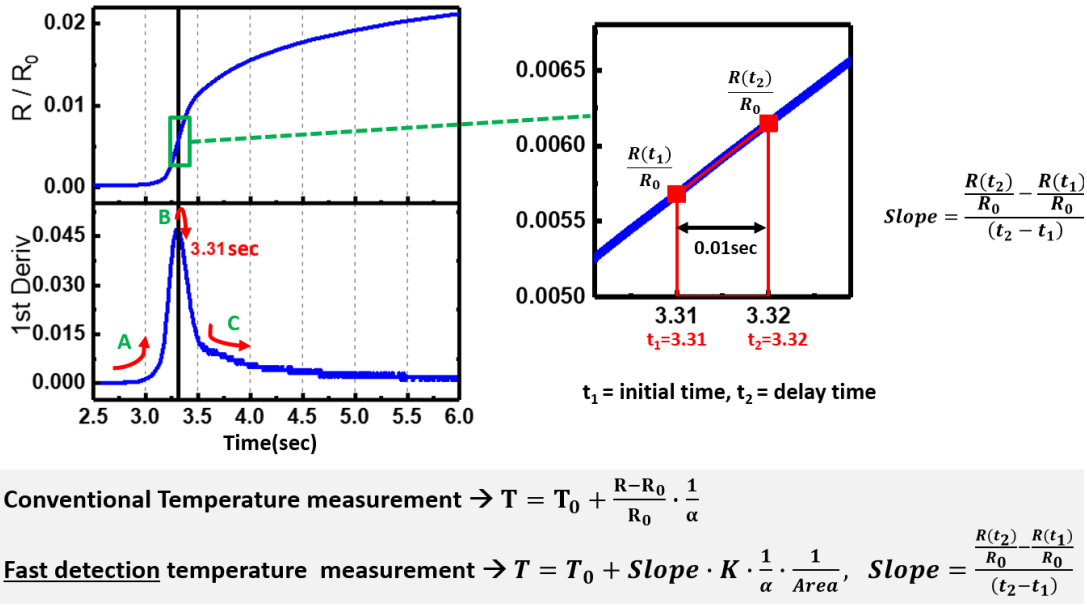

Fig 4.1.1.1 Principle of fast detection method measuring the variation slope. Before signal saturated, it is able to assume the temperature level measuring the deviation of before and after value of resistance.

the conventional method of capturing the point at which the temperature is kept constant, we propose a new method to determine the slope by capturing the point at which the resistance changes rapidly. Fig 4.1.1.1 introduces the 'Fast detection' method to measure the slope of the resistance change. A 2mm diameter tip was given a temperature of 60ºC, touched on the sensor, and collected time domain data and a first derivative graph through the SMU. The first derivative shows the slope of the resistance change. In part A, the residual heat emitted from the tip stimulates the sensor through air, and then shows the moment when the tip contacts the sensor and conducts heat. During the transition from A to B, the heat in contact with the sensor spreads in all directions. In part B, the maximum speed of temperature change is shown, and the saturation speed increases slowly as it moves to C. We decided to differentiate the temperature by capturing the most intuitively noticeable part of the slope (B). The time of part B was detected as 3.31 seconds, and the deviation of the resistance changes value after a certain time was calculated, and the slope formula is as follows

$$Slope = \frac{\frac{R(t_2)}{R_0} - \frac{R(t_1)}{R_0}}{t_2 - t_1} \quad (4.1.1.2)$$

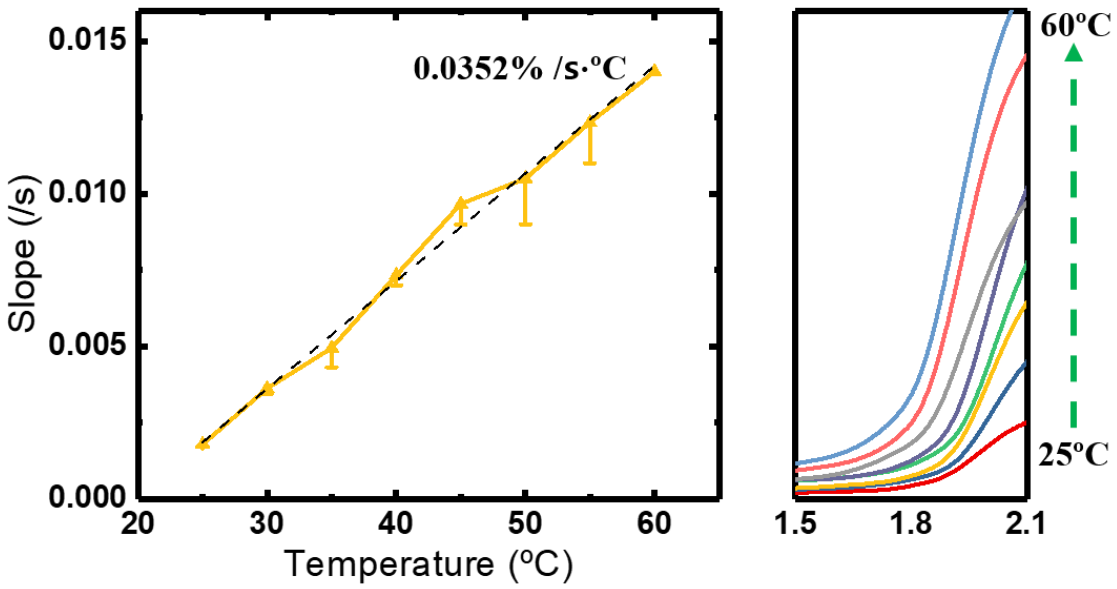

Fig 4.1.1.2 Temperature classification using fast detection method. From 25°C to 60°C, linear relationship between temperature and slope have been derived.

Where R_0, $R(t_1)$, $R(t_2)$, t_1, t_2 are the initial resistance value, resistance value at time t_1, t_2, time of deviation maximum value, time delayed from t_1. t_1 is 3.31 sec and R(3.31) is 8749Ω. Assuming that the delay from t1 to t2 is set to 0.01 seconds, t_2 will point to 3.32 sec, and the value of R(3.32) will be 8753 Ω. Given that R0 is 8700 Ω, the calculation result of slope came with, $\text{Slope} = \frac{1.00568-1.00615}{3.32-3.31[\text{sec}]} = \frac{0.00047}{0.01[\text{sec}]} = 0.047/\text{sec}$. Fig 4.1.1.2 shows the result of deriving the slope value according to the classified temperature value by using the fast detection method of a delay value of 0.01 seconds. This fact shows that the temperature and slope values have a linear relationship and proves that the level of thermal stimulation applied to the sensor can be classified. In the conventional temperature sensing equation, the sensitivity is derived from the temperature coefficient by detecting the changed resistance value based on the initial resistance value. From a similar point of view, the fast detection method

can determine the sensitivity through the difference in the speed of the resistance value. The measurement result has a sensitivity of 0.0352%/s per unit temperature.

When temperature is applied to a narrow area of a resistive single temperature sensor, the temperature spreads to the surroundings due to heat conduction. When thermal contact occurs on a temperature sensor that is limited in size, the intensity of the heat conduction direction is different for each pressure applied position. Fig 4.1.1.3(a) shows the slope size that appears when contact of 2mm diameter and 36ºC is applied to each point X, Y, Z. The Y point is located in the middle, unlike the X and Z points, so when heat is generated, heat is conducted in various directions. However, since the X and Z points are located in the corners, the direction of heat conduction cannot spread in all directions of 360º and proceeds with 90º. In the end, when heat is applied to the Y point, the resistance of the larger area than the X and Z points changes over time and the rate of change of the total resistance changes rapidly. After setting the 5-second delay as a parameter, the slope value is 0.000178/s at point Y, and 0.00011/s, 0.000103/s at X, Z respectively. Fig 4.1.1.3(b) shows the graph and the deviations of X, Y, and Z when the 5 second delay is set as a parameter for fast detection. If the stimulus is given to the center point Y, the resistance value increases at a remarkably fast speed, while the rate of increase at the points X and Z is less than that of Y. The 'Slope / Slope average' formula was used to compare the deviation of the slope of the three points. In Fig 4.1.1.3(c), a 0.01 second delay was set as a variable for fast detection and compared with the previous case. Fig 4.1.6(b) When checking the result of expanding the 5.5~6 second section of the graph, the values of the slopes of X, Y, and Z are 0.00103/s, 0.00114/s, and 0.0011/s, respectively, and relatively similar I can tell. As a result of using the 'Slope / Slope average' to derive the time domain results of three points, it can be seen that the deviation of the 5-second delayed variable is smaller than that of applying the fast detection formula. It can be seen that if smaller the delay time variable, the smaller the deviation value, and the sensor uniformity can be increased. However, due to the limitations of the measurement system, it is difficult to derive a value which is less than 0.01 seconds. But considering the tendency, the result can be estimated sufficiently.

(a)

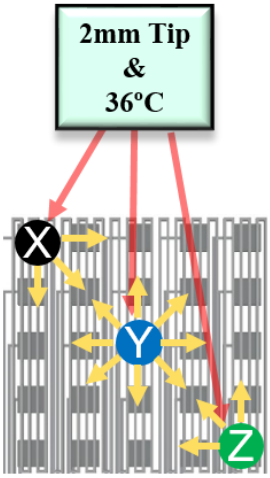

	Slope	
	5sec delay	0.01sec delay
X	0.00011 /s	0.00103 /s
Y	0.000178 /s	0.00114 /s
Z	0.000103 /s	0.0011 /s

(b) 5sec delay

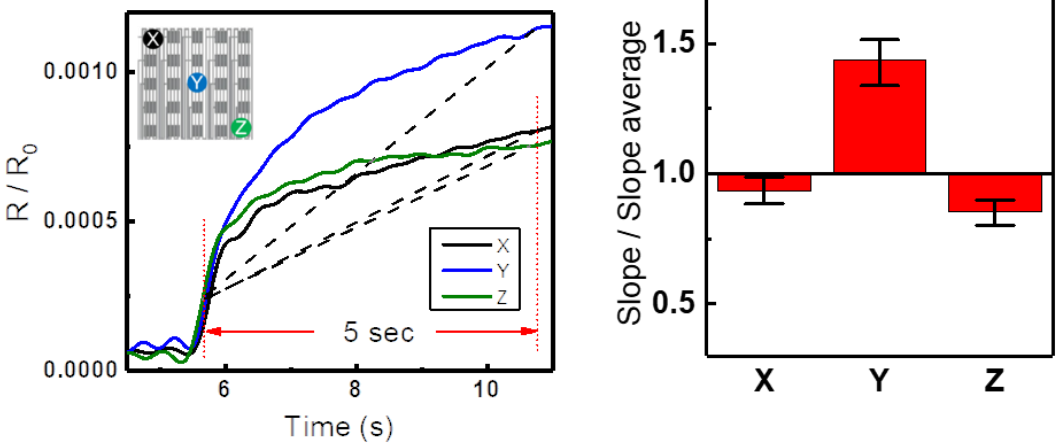

(c) 0.01sec delay

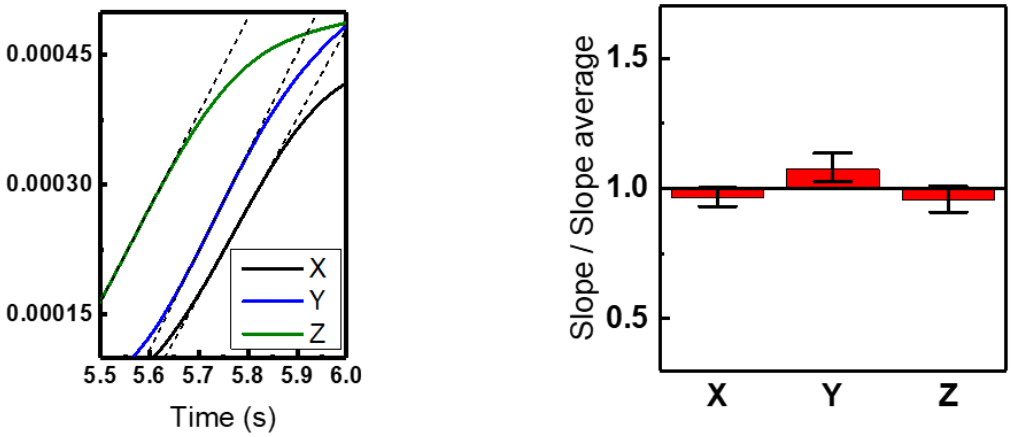

Fig 4.1.1.3 Uniformity test with varying the time delay parameter. (a) Testing the sample with contacting common condition at 3 different location on the sensor. (b) 0.01sec and (c) 5sec delay parameter results different deviation when comparing contacts of center and the corner.

4.1.2 Area classification

There is a second issue that it is difficult to distinguish if the area is different even if the same temperature are applied to the sensor. If so, there is a possibility that the problem can be solved by analyzing the tendency of resistance values with the fact that the change depends on the temperature and the contact area. If a pressure sensor of 25 cells is placed on the lower layer of the temperature sensor and a temperature sensor of single resistance type is divided into 25 cells, it can be analyzed after an one-to-one correspondence between each sensor cell. Fig 4.1.1.4 shows the analysis result by dividing a single resistance cell into 25 cells. It is possible to read the resistance change and the value of the touched micro piezoelectric sensor by applying to 1 and 4 cells respectively. However, the temperature sensor does not saturate when the resistance change value is analyzed in the time domain due to heat conduction, and the rate of increase is also different. Therefore, the resistance value changed from a single resistance cell R should not be interpreted as an approach that simply defines a constant value as R+a. For a value, the slope value using the fast detection method is appropriate, and the variable part of the conventional temperature resistance equation is replaced by a time domain function.

$$25R_0 + a = \sum_{i=1}^{25} R_0 + R_0(T_i - T_0)\alpha$$
$$= 25R_0 + \frac{R(t_2)-R(t_1)}{t_2-t_1}C \qquad (4.1.2.1)$$

Instead of adding the resistance values of each 25 cell as a sequence, we propose a method of expressing the additional resistance change in one equation. Fig 4.1.1.5 shows the temperature sensing procedure. When a stimulus of a specific resistance value slope, area, and temperature condition are applied to the sensor, the specific slope value and area information are collected by the pressure sensor and the resistance temperature sensor. In order to estimate the temperature using the area and slope information, the collected area information is appropriately searched for the data organized in a table. Among them, if you find the corresponding slope value and recognize the level of temperature, you can finally know the size of the

temperature applied to the sensor. Using multiple pressure sensors, we propose a mechanism that allows accurate temperature sensing despite having the same temperature but contacting different areas.

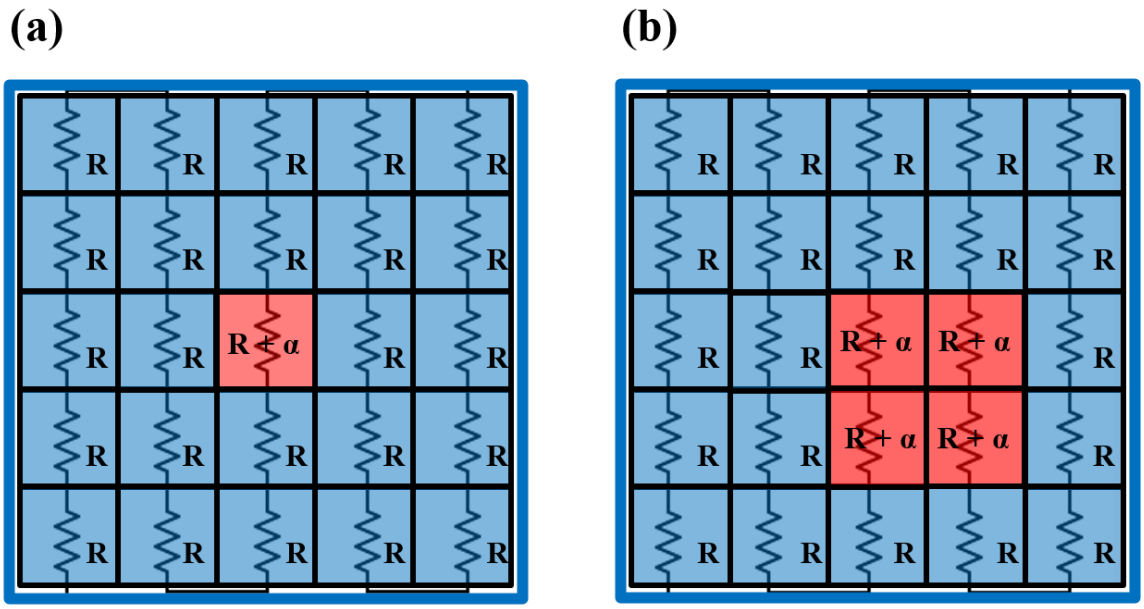

Fig 4.1.1.4 Schematic of system comparing two cases of different contact area. Pressure sensor below the temperature sensor supports area. Cell resistance behavior of conatacting (a) larger area contact and (b) smaller contact area.

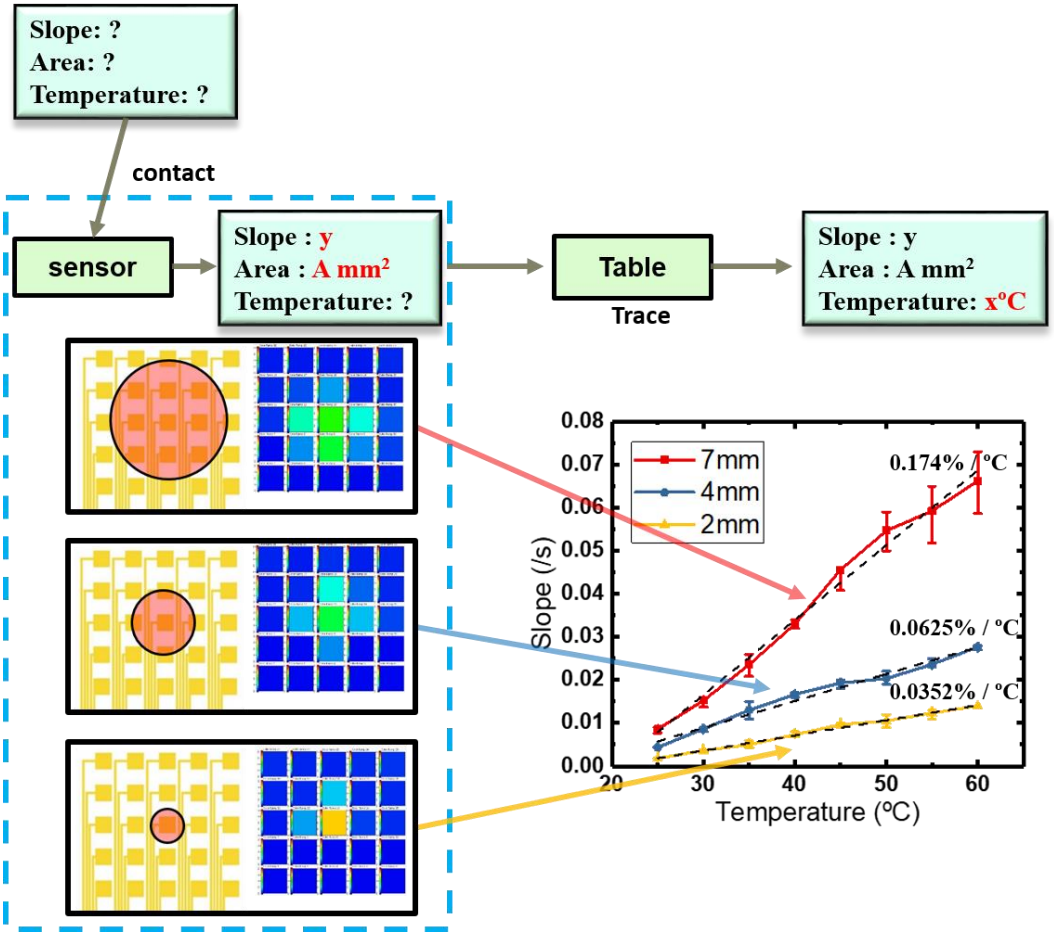

Fig 4.1.1.5 Temperature sensing flow using area information and slope result arrangement.

4.2 Pressure Sensor Signal

The pressure sensor is composed of 25 cells and is designed in a square shape with a side length of 1mm. In addition, the resolution is arranged at 1mm intervals, and the area of the stimulated area is proportional to the number of pressed cells. For example, if one cell is pressed, it is 1 x 1 mm^2, and if 4 cells are stimulated at the same time, it is possible to detect the stimulation of an area of 3 x 3 mm^2 considering the spacing. However, there are times when there are limitations in resolution. If pressure is applied to the middle of the four cells, the tip with an area enough to trigger one cell will activate the four cells. Due to this, it may be difficult to accurately determine the area of the stimulated pressure. In order to minimize this error, the piezoelectric element characteristics that are proportional to the applied area

and voltage were analyzed. An experiment was conducted in which various parts of the sensor were touched with a tip of a certain size(Fig 4.2.1). Fig. 4.2.1(a) shows the process of deriving the voltage by touching the 2mm diameter tip with a constant interval of 0.5mm and pressure from cells 1 to 5. For each cell, the voltage increases and decreases, and has a certain rule. If the tip touches one cell, it occurs the maximum value of the voltage. but if the tip touches two cells at the same time, the magnitude of the voltage is less than the maximum voltage value. To define these phenomena, we analyzed the phenomenon occurring in one piezoelectric cell by substituting a formula(Fig 4.2.1(b)). The piezoelectric cell capacitance formula is as follows

$$C = \frac{\varepsilon_r \varepsilon_0 \cdot Area_{cell}}{L} \tag{4.2.1}$$

where ε_0, ε_r $Area_{cell}$, L are the absolute permittivity, the dielectric constant of piezoelectric material, area of the cell and length of the cylinder, respectively. To induce polarization charges formula is as follows

$$Q = Area_{touch} \cdot \frac{F}{Area_{tip}} \cdot d \tag{4.2.2}$$

Where $Area_{tip}$, $Area_{touch}$, F, d are the contact area of the tip on the sensor surface, overlapped area of the tip and the piezoelectric cell, force, piezoelectric coefficient. Due to the thin thickness of the cell and the flexible substrate, even if the tip presses the cell, the $Area_{tip}$ value remains constant as long as the tip does not change. Therefore, the electric charge value has a proportional relationship with $Area_{touch}$, which means the section where the tip and the piezoelectric cell overlapped, and a different value is derived according to the condition of pressing the cell. The piezoelectric voltage derived by combining the capacitance value and the electric charge value has the following formula.

$$V = \frac{Q}{C} = \frac{Area_{touch} \cdot F \cdot d \cdot L}{\varepsilon_r \varepsilon_0 \cdot Area_{cell} \cdot Area_{tip}} \tag{4.2.3}$$

If the same force is applied without changing the tip, the voltage will change for each cell contact area, and it will depend on the $Area_{touch}$ value of formula (4.2.3). Except for this value, the rest of the variables hold a constant value, determine the area of an individual by

the size of the cell voltage, and derive the voltage information of each 25 cell to derive the voltage applied to the sensor. The black line in Fig 4.2.1(a) represents the total sum of the voltage values when piezoelectricity occurs in each section. Fig. 4.2.1(c) shows an experiment in which a voltage is derived by contacting cells 1 to 5 at 0.5mm intervals with tips of various areas(diameter 2mm~7mm) while maintaining a constant pressure. For tips with 2mm, 4mm, and 7mm diameters, even if the pressure is applied to various spaces with a sensor, areas can be classified. Fig 4.2.2 shows the result of collecting the actual data of the voltage peak of each cell by touching the center of the sensor with the same pressure with the tips and the summed value. Three contact conditions have been classified and can contribute to the results of the temperature sensor.

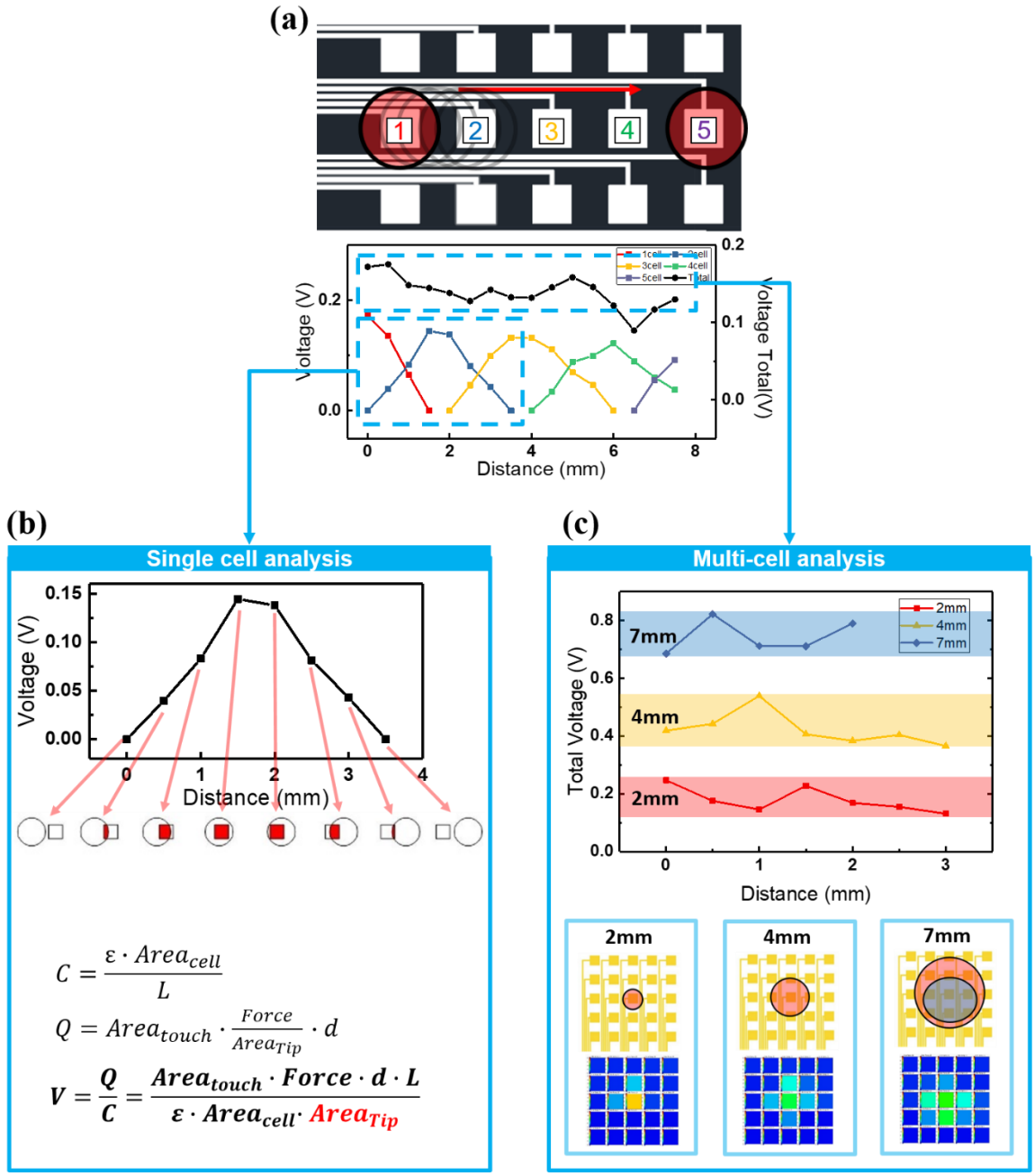

Fig 4.2.1 Schematic of classifying the touched area using pressure sensor. (a) Applying pressure from cell 1 to 5 with moving 0.5mm intervals. (b) Analyzing a cell with piezoelectric equation. (c) Classification of applied contact area with the tips (2mm, 4mm, 7mm).

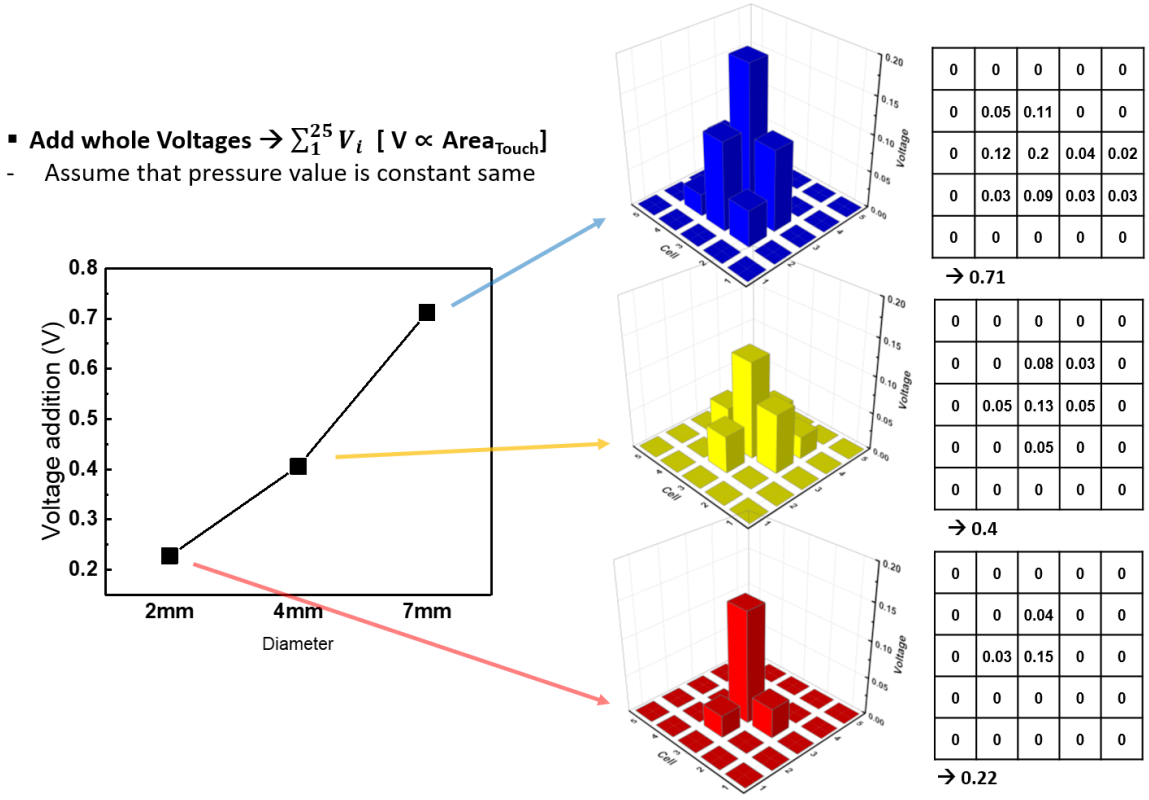

Fig 4.2.2 Detailed results of voltage level value with various contact diameter. Since the voltage magnitude of the pressure cell increases proportionally to the area where the cell and tip overlap, we add 25 voltage magnitudes.

4.3 Hybrid Sensor Signal

Previously, contact area values, resistance change rates, and temperature coefficient values were defined from temperature sensors and pressure sensors. In order to define temperature accurately, the interaction relationship between each parameter must be clearly defined. To define the relationship between the slope value collected from the temperature sensor and the temperature, follow relationship

$$T \propto Slope \tag{4.3.1}$$

which the temperature is proportional to slope value. Also, assuming the same temperature stimulus and considering the situation of different areas, the relationship between the sensing temperature and the area is

$$T \propto \frac{1}{Area_{touch}} \tag{4.3.2}$$

which the temperature is inverse proportional relationship. To define the rate of change of the detected temperature, the relationship between the area and the slope must be taken, and the relationship between them is

$$\Delta T \propto \frac{Slope}{Area_{touch}} \tag{4.3.3}$$

However, errors may occur when considering the thermal conductivity and resolution of the pressure sensor.

4.3.1 Equation analysis

To correct this, the overall formula is proposed in Fig 4.3.1.1(a) by adding a correction constant based on the experimental value. The relationship with temperature was established through the temperature coefficient α derived based on the conventional resistance equation theory, the area from the touchpad, and the slope from the resistance temperature sensor, and finally, the correction constant K is defined. Based on the data collected in Fig 4.1.1.5 through the experiment, it shows a method of deriving by tracking the correction constant K in reverse. Fig 4.3.1.1(b) shows the calculation process tracking inversely, and the K value is defined by classifying by the area of the applied tips(diameter: 2mm, 4mm, 7mm).

(a)

$$T = T_0 + Slope \cdot \frac{K}{\alpha \cdot \text{Area}}$$

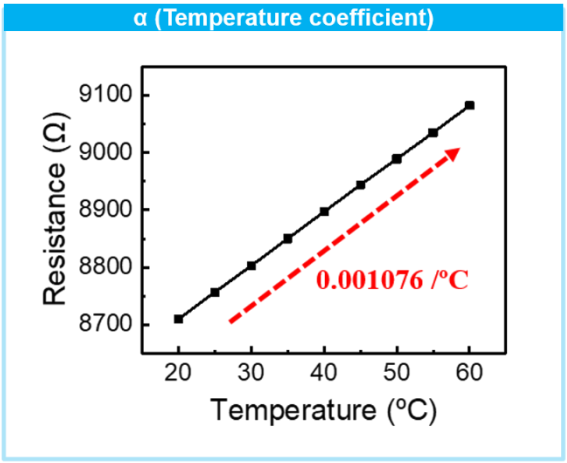

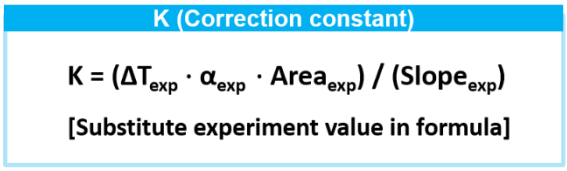

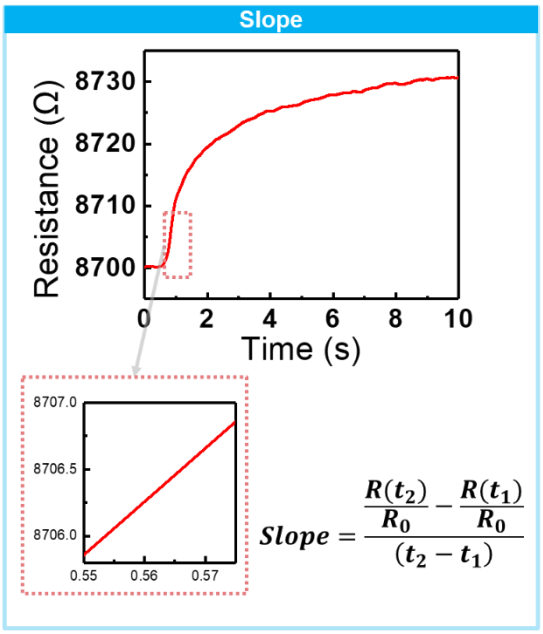

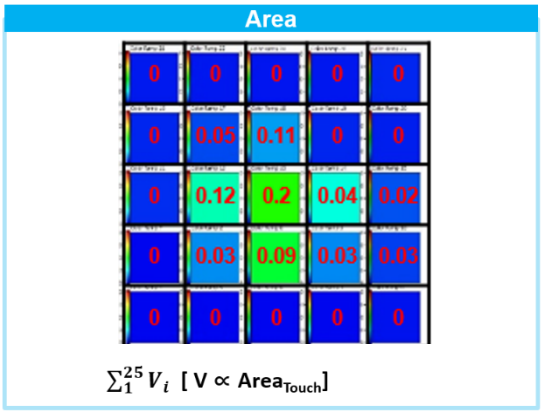

(b)

2mm	4mm	7mm
$\Delta t = 0.01\ sec$ α = 0.001076 /ºC Area = 0.22 $K = \frac{1}{n}\sum_1^n \frac{(\Delta T_n \times \alpha \times Area_{2mm})}{Slope_n}$ K = 0.6642V·s	$\Delta t = 0.01\ sec$ α = 0.001076 /ºC Area = 0.4 $K = \frac{1}{n}\sum_1^n \frac{(\Delta T_n \times \alpha \times Area_{4mm})}{Slope_n}$ K = 0.5565V·s	$\Delta t = 0.01\ sec$ α = 0.001076 /ºC Area = 0.71 $K = \frac{1}{n}\sum_1^n \frac{(\Delta T_n \times \alpha \times Area_{7mm})}{Slope_n}$ K = 0.4374V·s

Fig 4.3.1.1 Equation derived from integration of area and slope. (a) Slope defined with the parameters such as slope, temperature coefficient, area, correction constant. (b) Correction constant K derived with calculating reversly, based on experimental data.

4.3.2 Signal classification

Fig 4.3.2.1(a) shows the result of applying the sensor by temperature and tip area. 2mm~7mm diameter tips and a temperature condition of 30~50ºC is given, and an experiment was conducted to prove the uniformity. In the case of A, B, and C with a 2mm touch, they all touched one cell and touched another location in the sensor, but similar slope values were derived. Although the location is different, the temperature range of 10ºC is easily distinguished. Likewise, in the case of D~F and G~I, when 4, 6~7 cells are operated regardless of the touch position, the slope value is similarly detected and the applied temperature can be easily distinguished. Fig 4.3.2.1(b) is a table and summarized by measuring the slope value and the

(a)

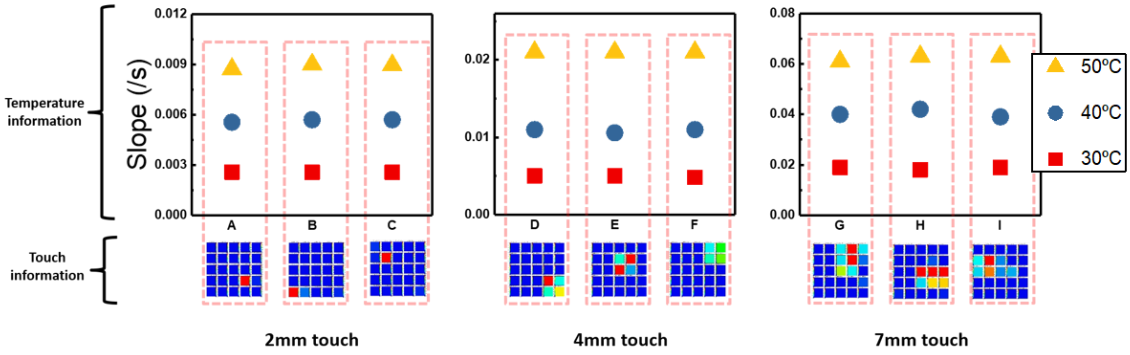

(b)

			Slope (/s)								
			0.0026/s	0.0057/s	0.009/s	0.005/s	0.01/s	0.022/s	0.018/s	0.04/s	0.062/s
Touch area	1 cell	A	29.2ºC	40.4ºC	52.3ºC						
		B	29.3ºC	39.9ºC	51.3ºC						
		C	29.3ºC	40.5ºC	52.2ºC						
	4cell	D				28.8ºC	39.4ºC	56.9ºC			
		E				28.8ºC	38.6ºC	56.9ºC			
		F				28.4ºC	39.4ºC	56.9ºC			
	6~7cells	G							29.6ºC	40.1ºC	50.8ºC
		H							29.1ºC	41.2ºC	51.8ºC
		I							29.6ºC	39.7ºC	51.8ºC

Resistance slope information + Touch area information

→ exact temperature value

Fig 4.3.2.1 Temperature sensing flow using area information and slope result arrangement.

area of the pressed cell. The same for A~C, 1cell + 0.00259/s represents 29.2ºC~29.3 ºC, 0.00556/s, 0.00571/s represents 39.9ºC~40.5 ºC, and 0.00873/s, 0.009/s, 0.00896/s represents 51.3ºC~52.3 ºC. For D~F, 4cell + 0.00485, 0.00502/s is 28.4 ºC~28.8ºC, 0.011/s, 0.01059ºC, is 38.6ºC~39.4 ºC, 0.021/s is 56.9ºC. For G~I, 6~7cell + 0.018/s, 0.019/s is 29.1ºC~29.6 ºC, 0.039/s~0.042/s is 39.7ºC~41.2ºC, 0.061/s, 0.063/s stands for 50.8ºC~51.8ºC. As a result, the exact temperature can be extracted by integrating the resistance gradient information and the touch area data using the formula.

Fig 4.3.2.2 shows through the table that case classification is possible when information about the same temperature or slope is collected utilizing. Fig 4.3.2.2(a) shows that the slopes of resistance sensor signal A, B, and C are 0.01/s, 0.01/s, and 0.016/s, respectively. In Fig. 4.3.2.2(b), when comparing A and B, the similar slope signal was collected, but area information (A: 0.22, B: 0.4) was applied as a piezoelectric voltage signal to distinguish 47.13ºC and 31.21ºC, respectively. In the case of B and C, the same temperature were stimulated, but different slope values and area information were derived and received. However, each can detect 31.21ºC, 29.16ºC, respectively, stimulation from the formula analysis. Fig. 4.3.2.2(c)(d) shows the process of interpreting the correct values using a formula even though approximate variables of A, B, and C were derived, respectively.

Fig 4.3.2.3 describes the application of the hybrid sensor to detect pain caused by overheating. Fig. 4.3.2.3(a) shows the process of detecting pain by collecting the slope information of 1 cell and resistance, combining the two information, and sensing a temperature of 45ºC. Fig. 4.3.2.3(b) shows the response speed and shows the process of obtaining the peak value of the pressure voltage and the delay value of the detected part of the slope through fast detection of the resistive temperature sensor. The response speed of the sensor was detected as 70msec, which is similar to the speed at which a human suffers through nerves(Fig 4.3.2.3(c)). It is defined as the reaction speed from the moment the device is stimulated to the moment the temperature sensor and the pressure sensor finish collecting information and mimics the nervous system A-delta that detects fast pain[49]. It is transmitted at a speed of 5~30m/sec, and the arrival time is assumed when the distance of the nervous system is assumed to be 1m.

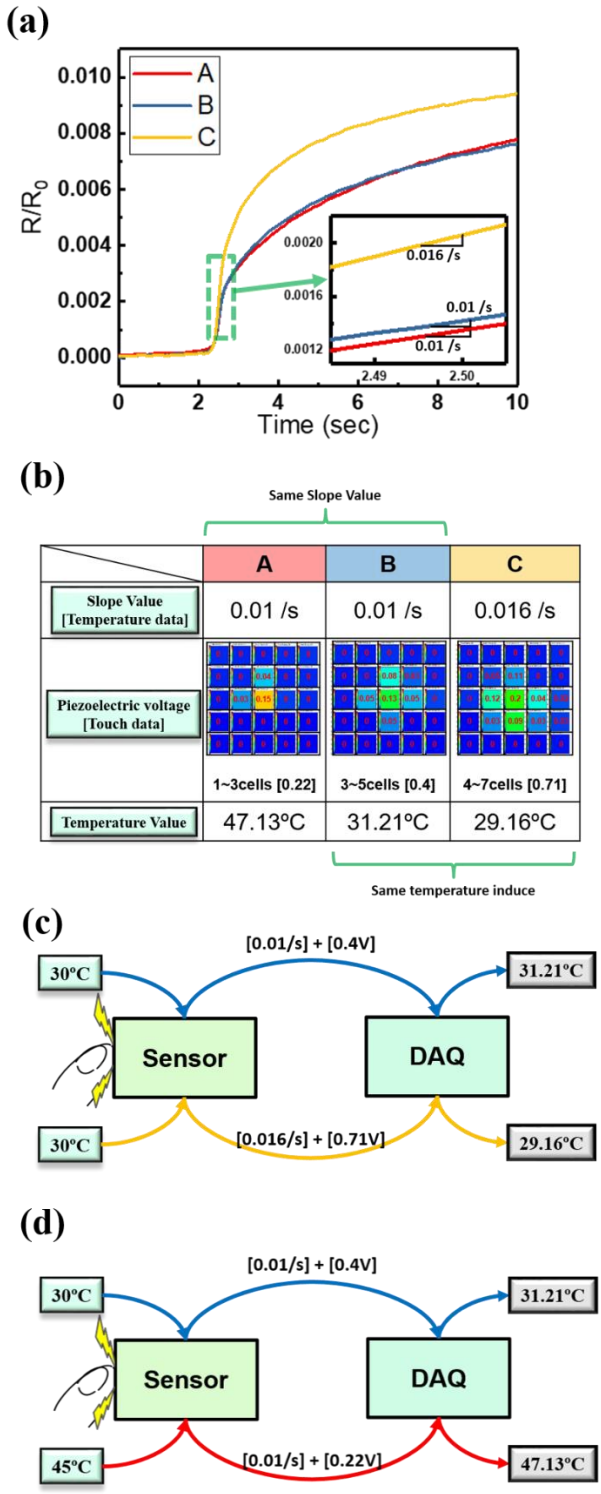

Fig 4.3.2.2 Same temperature stimulus and slope signal and measurement procedure. (a) Same temperature stimulus and slope signal. (b) measurement procedure. Resistance change signal and table data from cases A, B, and C. (c) Same temperature but different slope and area information. (d) Different temperatures but with the same slope.

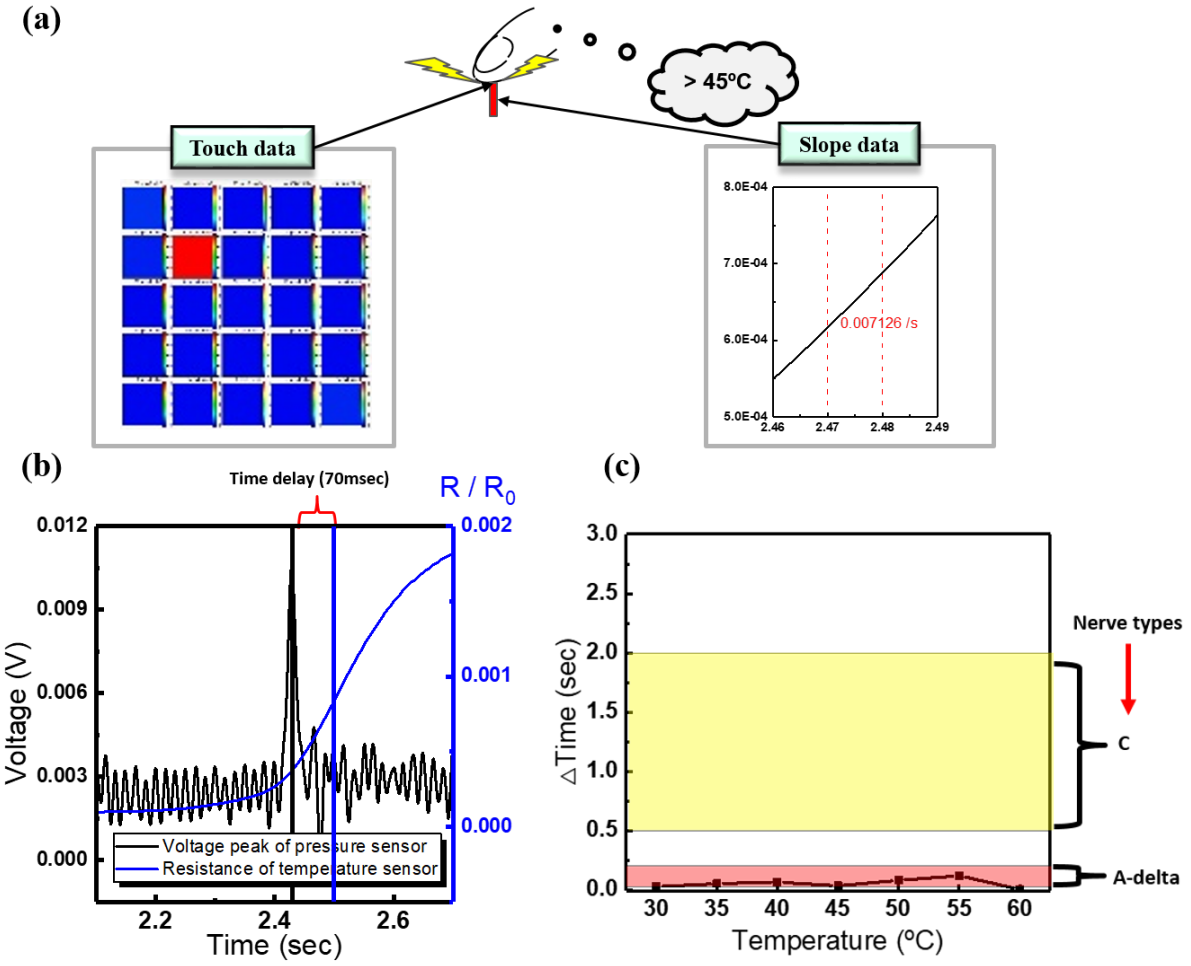

Fig 4.3.2.3 Using application of detecting the threaten of hot pain, up to 45°C.

Ⅴ. CONCLUSION

We propose a hybrid sensor that combines a temperature sensor using a single resistance sensor and a pressure sensor with 25 multi-array cell structures. The temperature sensor is composed of aluminum 100nm thick, 0.1mm wide and 30-40cm long, and is placed on the top layer to sensitively receive external stimuli. In addition, the resistance single temperature sensor can receive the resistance value of one element with the SMU, and the common ground electrode of the pressure sensor is deposited. Therefore, we have presented a way to solve the complexity of multi-sensing systems by simplifying the structure. The pressure sensor collects area information by making a piezoelectric sensor based on self-generation with PVDF-TrFE material. Also, under the assumption that the same pressure is applied to the piezoelectric material, the area information is collected by utilizing the property that the voltage level increases as the area increases. The hybrid sensor with an area of 1cm x 1cm detects the temperature using the conventional temperature resistance equation like a general temperature sensor when it is stimulated over a large area, but when it receives a stimulus over a smaller area, a new method for sensing temperature must be found. Compared to a hybrid sensor that combines a pressure sensor and a temperature sensor, the stimulus of a narrower area is compensated for the thermal stimulus detection result of the temperature sensor by grasping the size of the contact object with 25 piezoelectric sensor cells with relatively high resolution. In addition, fast detection was used to propose a solution to the problem that the resistance change was difficult to saturate due to the heat conduction problem. Among the parameters, the shorter the delay time, the more uniform characteristics of the stimulus position became, and information collection became possible in a short time. Through this, it is possible to collect temperature and pressure information within 70msec of reaction speed. Finally, we analyzed the phenomenon by analyzing the trend of the signal received by each sensor and establishing a formula. It also detects the stimulated conditions using a table that summarizes the values of temperature and slope. We propose a trick to solve the complexity of the multi-sensing skin system through the simplified hybrid sensor structure.

References

[1] Chortos, Alex, Jia Liu, and Zhenan Bao. "Pursuing prosthetic electronic skin." *Nature materials* 15.9 (2016): 937-950.

[2] Yang, Tingting, et al. "Recent advances in wearable tactile sensors: Materials, sensing mechanisms, and device performance." *Materials Science and Engineering: R: Reports* 115 (2017): 1-37.

[3] Yu, Junbin, et al. "Highly skin-conformal wearable tactile sensor based on piezoelectric-enhanced triboelectric nanogenerator." *Nano Energy* 64 (2019): 103923.

[4] Jeong, Yeri, et al. "Psychological tactile sensor structure based on piezoelectric nanowire cell arrays." *RSC Advances* 5.50 (2015): 40363-40368.

[5] Shin, Kwonsik, et al. "Artificial Tactile Sensor With Pin-type Module for Depth Profile and Surface Topography Detection." *IEEE Transactions on Industrial Electronics* 67.1 (2019): 637-646.

[6] Wang, Xiandi, et al. "Full Dynamic-Range Pressure Sensor Matrix Based on Optical and Electrical Dual-Mode Sensing." *Advanced Materials* 29.15 (2017): 1605817.

[7] Chun, Sungwoo, et al. "Self-powered pressure-and vibration-sensitive tactile sensors for learning technique-based neural finger skin." *Nano letters* 19.5 (2019): 3305-3312.

[8] Lai, Ying-Chih, et al. "Entirely, Intrinsically, and Autonomously Self-Healable, Highly Transparent, and Superstretchable Triboelectric Nanogenerator for Personal Power Sources and Self-Powered Electronic Skins." *Advanced Functional Materials* 29.40 (2019): 1904626.

[9] Niu, Hongsen, et al. "Highly Morphology-Controllable and Highly Sensitive Capacitive Tactile Sensor Based on Epidermis-Dermis-Inspired Interlocked Asymmetric-Nanocone Arrays for Detection of Tiny Pressure." *Small* 16.4 (2020): 1904774.

[10] Qiu, Jie, et al. "Rapid-response, low detection limit, and high-sensitivity capacitive flexible tactile sensor based on three-dimensional porous dielectric layer for wearable electronic skin." *ACS applied materials & interfaces* 11.43 (2019): 40716-40725.

[11] Wang, Chunya, et al. "An all-silk-derived dual-mode E-skin for simultaneous temperature–pressure detection." *ACS applied materials & interfaces* 9.45 (2017): 39484-39492.

[12] Gong, Shu, et al. "Local Crack-Programmed Gold Nanowire Electronic Skin Tattoos for In-Plane Multisensor Integration." *Advanced Materials* 31.41 (2019): 1903789.

[13] Guo, Ying, et al. "A wearable transient pressure sensor made with MXene nanosheets for sensitive broad-range human–machine interfacing." *Nano letters* 19.2 (2019): 1143-1150.

[14] Ma, Mingyuan, et al. "Self-powered flexible antibacterial tactile sensor based on triboelectric-piezoelectric-pyroelectric multi-effect coupling mechanism." *Nano Energy* 66 (2019): 104105.

[15] Tien, Nguyen Thanh, et al. "A flexible bimodal sensor array for simultaneous sensing of pressure and temperature." *Advanced Materials* 26.5 (2014): 796-804.

[16] Sim, Minkyung, et al. "Electronic Skin to Feel “Pain”: Detecting “Prick” and “Hot” Pain Sensations." *Soft Robotics* 6.6 (2019): 745-759.

[17] Xin, Yangyang, Jian Zhou, and Gilles Lubineau. "A highly stretchable strain-insensitive temperature sensor exploits the Seebeck effect in nanoparticle-based printed circuits." *Journal of Materials Chemistry A* 7.42 (2019): 24493-24501.

[18] An, Byeong Wan, et al. "Transparent and flexible fingerprint sensor array with multiplexed detection of tactile pressure and skin temperature." *Nature communications* 9.1 (2018): 1-10.

[19] Webb, R. Chad, et al. "Ultrathin conformal devices for precise and continuous thermal characterization of human skin." *Nature materials* 12.10 (2013): 938-944.

[20] Zhao, Shuai, and Rong Zhu. "Electronic skin with multifunction sensors based on thermosensation." *Advanced Materials* 29.15 (2017): 1606151.

[21] Zhang, Fengjiao, et al. "Flexible and self-powered temperature–pressure dual-parameter sensors using microstructure-frame-supported organic thermoelectric materials." *Nature communications* 6.1 (2015): 1-10.

[22] Tien, Nguyen Thanh, et al. "A flexible bimodal sensor array for simultaneous sensing of pressure and temperature." *Advanced Materials* 26.5 (2014): 796-804.

[23] Kim, Jaemin, et al. "Stretchable silicon nanoribbon electronics for skin prosthesis." *Nature communications* 5.1 (2014): 1-11.

[24] Hu, Hongjie, et al. "Stretchable ultrasonic transducer arrays for three-dimensional imaging on complex surfaces." *Science advances* 4.3 (2018): eaar3979.

[25] Kurilova, L. M., and S. L. Bliakher. "Properties of cold receptors." *Bulletin of Experimental Biology and Medicine* 45.4 (1958): 403-406.

[26] Park, Minhoon, et al. "Recent advances in tactile sensing technology." *Micromachines* 9.7 (2018): 321.

[27] Yang, Y-J., et al. "A 32× 32 temperature and tactile sensing array using PI-copper films." *The International Journal of Advanced Manufacturing Technology* 46.9-12 (2010): 945-956.

[28] Ma, Zhong, et al. "Advanced electronic skin devices for healthcare applications." *Journal of Materials Chemistry B* 7.2 (2019): 173-197.

[29] https://en.wikipedia.org/wiki/Somatosensory_system

[30] Abraira, Victoria E., and David D. Ginty. "The sensory neurons of touch." *Neuron* 79.4 (2013): 618-639.

[31] https://courses.lumenlearning.com/boundless-biology/chapter/somatosensation/

[32] Eliav, Eli, and Richard H. Gracely. "Measuring and assessing pain." *Orofacial pain and headache. Philadelphia, PA: Elsevier Health Sciences* (2008): 45-56.

[33] Lee, Hyunjae, et al. "Wearable/disposable sweat-based glucose monitoring device with multistage transdermal drug delivery module." *Science advances* 3.3 (2017): e1601314.

[34] Shin, Kwonsik, et al. "Artificial tactile sensor structure for surface topography through sliding." *IEEE/ASME Transactions on Mechatronics* 23.6 (2018): 2638-2649.

[35] Puers, B., et al. "A capacitive pressure sensor with low impedance output and active suppression of parasitic effects." *Sensors and Actuators A: Physical* 21.1-3 (1990): 108-114.

[36] Wan, Yongbiao, et al. "A Highly Sensitive Flexible Capacitive Tactile Sensor with Sparse and High-Aspect-Ratio Microstructures." *Advanced Electronic Materials* 4.4 (2018): 1700586.

[37] Maiolino, Perla, et al. "A flexible and robust large scale capacitive tactile system for robots." *IEEE Sensors Journal* 13.10 (2013): 3910-3917.

[38] Wan, Yongbiao, Yan Wang, and Chuan Fei Guo. "Recent progresses on flexible tactile sensors." *Materials Today Physics* 1 (2017): 61-73.

[39] Wu, Chaoxing, et al. "Self-Powered Tactile Sensor with Learning and Memory." *ACS nano* 14.2 (2019): 1390-1398.

[40] Wang, Xiandi, et al. "Recent progress in electronic skin." *Advanced Science* 2.10 (2015): 1500169.

[41] Graz, Ingrid, et al. "Flexible active-matrix cells with selectively poled bifunctional polymer-ceramic nanocomposite for pressure and temperature sensing skin." *Journal of Applied Physics* 106.3 (2009): 034503.

[42] Tien, Nguyen Thanh, et al. "Utilizing highly crystalline pyroelectric material as functional gate dielectric in organic thin-film transistors." *Advanced Materials* 21.8 (2009): 910-915.

[43] Dankoco, M. D., et al. "Temperature sensor realized by inkjet printing process on flexible substrate." *Materials Science and Engineering: B* 205 (2016): 1-5.

[44] Shin, Jaeho, et al. "Sensitive Wearable Temperature Sensor with Seamless Monolithic Integration." *Advanced Materials* 32.2 (2020): 1905527.

[45] Zhao, Shuai, and Rong Zhu. "Electronic skin with multifunction sensors based on thermosensation." *Advanced Materials* 29.15 (2017): 1606151.

[46] Hua, Qilin, et al. "Skin-inspired highly stretchable and conformable matrix networks for multifunctional sensing." *Nature communications* 9.1 (2018): 1-11.

[47] Gautschi, Gustav. "Piezoelectric sensors." *Piezoelectric Sensorics*. Springer, Berlin, Heidelberg, 2002. 73-91.

[48] Tajitsu, Y., et al. "Crystalline phase transition in the copolymer of vinylidenefluoride and trifluoro-ethylene." *Applied Physics Letters* 36.4 (1980): 286-288.

[49] Dubin, Adrienne E., and Ardem Patapoutian. "Nociceptors: the sensors of the pain pathway." *The Journal of clinical investigation* 120.11 (2010): 3760-3772.

[50] https://biologyboom.com/write-a-note-on-mechanoreceptors-tactile-receptors-in-the-skin/

요 약 문

열 감지를 위한 압력 및 온도 하이브리드 시스템 기반 인공 촉각 센서

인간의 오감 모방은 과거부터 인간들에게 있어 가장 흥미로운 연구이다. 시각을 모방하기 위한 텔레비전과 카메라, 청각을 모방하기 위한 오디오와 마이크로폰, 후각 모방을 위한 가스 센서 등 현재 여러 모방을 통한 상품들이 일상생활에 사용되고 있다. 그러나 촉각 모방에 관한 연구 중 해결해야 하는 과제들이 많습니다. 현재, 인간의 촉각을 모방하기 위해 다양한 유형의 감지 방식을 갖춘 인공 촉각 센서가 많은 연구자에 의해 개발되고 있다. 촉각센서의 다양한 기술들은 로봇 보철물, 인간/기계 인터페이스, 바이오 메디컬 센서에 활용하기 위해 여러 방법을 연구 중이다. 특히 온도와 압력은 인간의 촉각에 있어 가장 중요한 요소 중의 하나이며, 피부 상태에 대한 유용한 정보를 제공한다. 또한, 이 두 가지 감각은 인간 피부의 기본 모방 변수로서 이를 조합하여 활용하면 통증, 진동, 경도 등의 고급 감각에 적용할 수 있으며, 다른 물체들과 효과적으로 교감할 수 있다. 촉각 모방을 실현하는 과정에서 최근 재료, 센서의 설계, 작동 메커니즘들을 고려하여 많은 유형의 방법이 연구되어 왔다. 또한, 시스템에 2 가지 이상의 센서를 통합하여 다양한 외부 자극을 감지할 수 있으며, 이상적인 인간의 느낌을 구현할 수 있다. 압력, 온도, 습도, 변형 등 여러 감각을 한 시스템에 효과적으로 집적하여 다중 감지를 실현하고 있다. 우선 많은 수의 센서를 사용해 다양한 외부 자극을 측정하려면 우선 구조적으로 복잡성을 고려해야 합니다. 다중감지 구조로 인해 센서를 집적하게 되면 센서의 수가 많아지게 되고, 그로 인해서 수신해야 하는 신호도 증가하게 된다. 또한, 복잡한 구조를 구현하기 위해 소자 공정 과정에 있어 막대한 비용이 요구된다. 뿐만 아니라 외부 자극 때문에 원하지 않는 변수들을 감지하게 되는 디커플링 효과가 발생한다. 이 논문에서는 다중 감지 구조를 단순화하여 온도와 터치를 감지할 수 있는 하이브리드 인공 촉각 센서를 제안한다. 단일 저항식 온도센서를 통해 구조를 간단화 시키고 25 개의 압전소자 활용을 통해 에너지 효율을 극대화했다. 이는 온도 센서보다 면적이 좁은 영역도 열이 인가되면 감지할 수 있으며, 새로운 공식과 메커니즘을 활용해 단순화된 센서의 장점을 활용한다. 인간 피부의 핵심 수용체인 기계수용체와 열수용체를 온도 센서와 압력 센서로 구현해 사람의 촉각 수용체들을 모방하는 데에 의미가 있다. 또한, 인간 피부 모방을 위한 다중 감지 시스템을 복잡성을 완화할 해결책을 제시하는 데에 의미가 있다.

핵심어: 촉각센서, 피에조, 저항식 온도센서, 다중 감지 시스템